Published in final edited form as:
Prog Retin Eye Res. 2009 May ; 28(3): 206–226. doi:10.1016/j.preteyeres.2009.04.004.

Functional Roles of Bestrophins in Ocular Epithelia

Alan D. Marmorstein[a,b,*], **Harold E. Cross**[a], and **Neal S. Peachey**[c,d,e]

[a] Department of Ophthalmology and Vision Science, University of Arizona, Tucson, AZ 85711 USA

[b] College of Optical Sciences, University of Arizona, Tucson, AZ 85711 USA

[c] Cole Eye Institute, Cleveland Clinic Foundation, Cleveland, OH 44195 USA

[d] Research Service, Cleveland VA Medical Center, Cleveland, OH 44106 USA

[e] Department of Ophthalmology, Cleveland Clinic Lerner College of Medicine of Case Western Reserve University, Cleveland, OH 44106 USA

Abstract

There are four members of the bestrophin family of proteins in the human genome, of which two are known to be expressed in the eye. The gene *BEST1* (formerly *VMD2*) which encodes the protein bestrophin-1 (Best1) was first identified in 1998. Mutations in this gene have now been associated with four clinically distinguishable human eye diseases, collectively referred to as "bestrophinopathies". Over the last decade, laboratories have sought to understand how Best1 mutations could result in eye diseases that range in presentation from macular degeneration to nanophthalmos. The majority of our knowledge comes from studies that have sought to understand how Best1 mutations or dysfunction could induce the classical symptoms of the most common of these diseases: Best vitelliform macular dystrophy (BVMD). BVMD is a dominant trait that is characterized electrophysiologically by a diminished electrooculogram light peak with a normal clinical electroretinogram. This together with the localization of Best1 to the retinal pigment epithelium (RPE) basolateral plasma membrane and data from heterologous expression studies, have led to the proposal that Best1 generates the light peak, and that bestrophins are a family of Ca^{2+} activated Cl^- channels (CaCCs). However, data from *Best1* knock-out and knock-in mice, coupled with the recent discovery of a recessive bestrophinopathy suggest that Best1 does not generate the light peak. Recently Best2 was found to be expressed in non-pigmented epithelia in the ciliary body. However, aqueous dynamics in *Best2* knock-out mice do not support a role for Best2 as a Cl^- channel. Thus, the purported CaCC function of the bestrophins and how loss of this function relates to clinical disease needs to be reassessed. In this article, we examine data obtained from tissue-type and animal models and discuss the current state of bestrophin research, what roles Best1 and Best2 may play in ocular epithelia and ocular electrophysiology, and how perturbation of these functions may result in disease.

1. Introduction

Mutations in the gene *BEST1*, encoding the protein Best1, cause a variety of degenerative eye diseases in man (Hartzell *et al.*, 2008a; Marmorstein and Kinnick, 2007). Since its

*Corresponding Author at Department of Ophthalmology and Vision Science, P.O. Box 245216, Tucson, AZ 85719-4215, USA, Tel: +1 520-626-0449; Fax: +1 520-626-0457; e-mail address: amarmorstein@eyes.arizona.edu.

identification, Best1 has become both the namesake of, as well as the prototypic member of the bestrophin family of proteins. The function of the bestrophins is a controversial subject. Bestrophins have been hypothesized to be a family of Ca^{2+} activated Cl^- channels (CaCCs), regulators of ion transport, or both (Hartzell *et al.*, 2005; Hartzell *et al.*, 2008a; Marmorstein and Kinnick, 2007; Sun *et al.*, 2002). The majority of studies on bestrophins have examined their putative Cl^- channel activity, and evidence for these functions in heterologous expression systems is compelling. Complementary evidence for this function in tissue is, however, lacking. As a result, the "CaCC hypothesis" has not met with broad acceptance, and the recent identification of the TMEM16 family of proteins as CaCCs (Caputo et al., 2008; Schroeder et al., 2008; Yang et al., 2008) has served to reinforce these doubts (Hartzell et al., 2008b). Based on data from animal models and tissue culture, we and others have suggested that bestrophins are regulators of ion transport rather than ion channels (Burgess *et al.*, 2008b; Hartzell *et al.*, 2008a; Marmorstein and Kinnick, 2007; Marmorstein *et al.*, 2006; Rosenthal *et al.*, 2006; Yu *et al.*, 2008). For those who wish a more detailed review of the literature pertaining to bestrophins as Cl^- channels we would direct the reader to the excellent reviews by Hartzell and co-workers (Hartzell et al., 2005; Hartzell et al., 2008a). Our goal in this article is to summarize the evidence in support of the hypothesis that bestrophins function as ion channel regulators. As such, we will review research on bestrophins with an emphasis on animal models and disease and contrast them with findings obtained in heterologous expression systems.

The identification of human Best1 resulted from identification of the gene responsible for Best vitellform macular dystrophy (BVMD). Originally designated *VMD2*, the *BEST1* gene was independently identified by two groups in 1998 (Marquardt et al., 1998; Petrukhin et al., 1998). The name 'bestrophin' was proposed by Petrukhin and colleagues (Petrukhin et al., 1998). Shortly thereafter, three human bestrophin paralogues were identified by Stohr and co-workers (Stohr et al., 2002). These genes were originally designated *VMD2L1, VMD2L2*, and *VMD2L3*. A subsequent revision of the genetic nomenclature by the HUGO gene nomenclature committee has resulted in the genes *VMD2, VMD2L1*, and *VMD2L3* being re-designated *BEST1, BEST2*, and *BEST3* respectively, with *VMD2L2* re-designated *BEST4*. The encoded paralogous proteins are also designated numerically, bestrophin-1 through bestrophin-4, abbreviated Best1 through Best4. When referring to bestrophins, species is often designated by a small case letter such that human bestrophin-1 is referred to as hBest1, mouse bestrophin-2 is indicated as mBest2, and so on.

Bestrophins are found across the animal kingdom with representatives identified in both eukaryotic and prokaryotic genomes (Hagen et al., 2005; Hartzell et al., 2008a; Milenkovic et al., 2008). In fact, the first identification of bestrophins resulted from the sequencing of the *Caenorhabditis elegans* genome which contains 25 distinct members of the gene family (Petrukhin et al., 1998). The *C. elegans* bestrophins were originally termed the RFP (or RFP-TM) family because computational analysis indicated that all contain a highly conserved group of aromatic amino acids including the sequence RFP (Arg-Phe-Pro). The lack of homology to other genes/proteins provided few clues to their prospective functions, though one group postulated that bestrophins may function as ion exchangers due to modest homology to retinal Na^+, K^+/Ca^{2+} exchangers (Gomez et al., 2001). *C. elegans* appears to be unique in the number and diversity of their bestrophin genes; most other species regardless of phylogenic classification have 4 or fewer. Mammalian genomes appear to have 4 members of the family corresponding to the 4 paralogous groups. Computer assisted analysis of bestrophins allows their primary sequence to be divided into two domains. The first of these constitutes the RFP or bestrophin domain, which contains the RFP motif, as well as several putative transmembrane (TM) domains, and extends from the N-terminal through the first ~350 amino acids (Bakall *et al.*, 1999; Hartzell *et al.*, 2005; Milenkovic *et al.*, 2007; Petrukhin *et al.*, 1998; Stanton *et al.*, 2006; Stohr *et al.*, 2002; Tsunenari *et al.*, 2003). This domain defines the protein as a member of the bestrophin family and is therefore very highly conserved; 26% between man

and bacteria The second “cytoplasmic” domain comprises the remaining protein through the C-terminus, and is conserved within paralogous groups, though poorly (Hartzell et al., 2008a). More information on the phylogenetic relationships among bestrophins can be found in a recent review by Milenkovic and co-workers (Milenkovic et al., 2008).

Since its discovery, Best1 has become the prototypic member of the bestrophin family of proteins, and to date most structural studies have focused on either hBest1 or mBest2. Bestrophins are integral membrane proteins as demonstrated by detergent phase partitioning in Triton X-114 (Marmorstein et al., 2000). Various computer-assisted hydropathy analyses have predicted that hBest1 has between 4 and 6 potential TM segments (Bakall *et al.*, 1999; Milenkovic *et al.*, 2007; Petrukhin *et al.*, 1998; Qu *et al.*, 2003; Tsunenari *et al.*, 2003; White *et al.*, 2000). Two studies have attempted to experimentally determine the membrane topology of hBest1 (Milenkovic *et al.*, 2007; Tsunenari *et al.*, 2003). Both concluded that the protein has 4 membrane spanning regions (Fig. 1A). Tsunenari *et al.* (2003) examined the topology of hbest1 TM domains by insertion of N-glycosylation sites and tobacco etch virus protease cleavage sites while Milenkovic et al., (2007) used the *in vitro* translation/translocation *Escherichia coli* leader peptidase (*Lep*) gene assay. Both studies concluded that TM1, TM2, and TM6 traverse the membrane, but disagreed on the topology of TM 4 and TM5. Tsunenari *et al.* (2003) suggested that TM4 but not TM5 spans the membrane while Milenkovic *et al.* (2007) proposed that TM4 was most likely intracellular and TM5 spans the membrane. While there is no experimental evidence favoring one model over the other, most studies in which a structure is proposed or discussed have used a model similar to that of Milenkovic *et al.* (2007). Using this model, the majority of disease causing mutations occur in clusters adjacent to or within the TM domains (Fig. 1B).

Bestrophin oligomers were first reported by Sun *et al.* (2002) in transfected HEK293 cells. However, we (Stanton et al., 2006) have demonstrated that the tetramers and pentamers observed by Sun *et al.* (2002) were due to aggregation of the over-expressed protein, a possibility acknowledged by those authors. Velocity sedimentation studies in our lab have demonstrated that porcine Best1 (pBest1) forms dimers when extracted from tissue using Triton X-100 (Stanton et al., 2006), the same detergent used by Sun *et al.* (2002). The protein binds a significant amount of detergent (0.48 ± 0.24 g Tx-100 / g protein) as would be expected from an integral membrane protein with multiple TM domains (Stanton et al., 2006). Dimeric pBest1 has a $S_{20,w}$ of 4.9 and a Stokes radius of 7.3nM (Stanton et al., 2006). As stated earlier, when overexpressed in cultured cells Best1 has a tendency to aggregate and collect within the cell, confounding efforts to study its quaternary structure. These data do not rule out the possibility that Best1 dimers may form higher order oligomers, but to date they have not been observed in native tissue extracts. The ability of Best1 to oligomerize has also led to speculation that bestrophins may form hetero-oligomers (Hartzell et al., 2005; Hartzell et al., 2008a). Again, however, bestrophin hetero-oligomers have not been observed in native tissue extracts, and the relatively restricted pattern of bestrophin protein expression would indicate that such oligomers only occur under certain laboratory conditions.

2. Tissue Distribution of Bestrophins

Both Petrukhin *et al.* (1998) and Marquardt *et al.* (1998) examined the distribution of *BEST1* mRNA in humans by Northern blot. Petrukhin *et al.* (1998) found expression in retina/RPE, brain, spinal cord, and testis. Marquardt et al. (1998) identified hBest1 mRNA only in retina/RPE and the human RPE-derived cell line ARPE-19. The hypothesis that bestrophins function as CaCCs has caused many investigators to examine Best1 expression in tissues with known CaCC activity. As a result, Best1 mRNA has been identified by two groups in trachea (Barro Soria et al., 2006; Duta et al., 2006), and by Barro-Soria *et al.*, (2006) in kidney and other epithelia using RT-PCR. The discrepancy between the PCR and Northern Blot data may rest

with the exquisite sensitivity of RT-PCR, which can detect extraordinary low levels of mRNA. However, even high levels of mRNA expression cannot be taken as evidence of protein expression. The human RPE derived cell lines ARPE-19 and D407, for example, both transcribe hBest1 mRNA, but neither cell line makes hBest1 protein (Marmorstein et al., 2000). In tissue, quantitative RT-PCR has shown high levels of Best1 mRNA in mouse embryonic eyes as early as E15, but we did not detect mBest1 protein until postnatal day 10 (Bakall et al., 2003).

The determination of protein expression requires the use of well characterized antibodies. We reported monoclonal (E6-6 and E6-1) and polyclonal (Pab-125) antibodies raised against the peptide KDHMDPYWALENRDEAHS, corresponding to the C-terminus of hBest1 (Marmorstein et al., 2000). These antibodies have been demonstrated to recognize primate (human and non-human), porcine, and canine Best1 (Guziewicz *et al.*, 2007; Marmorstein *et al.*, 2000; Marmorstein *et al.*, 2002; Mullins *et al.*, 2005). Using these antibodies, our laboratory demonstrated that Best1 protein is expressed by and localized to the basolateral plasma membrane of the RPE in macaque and porcine eyes (Marmorstein et al., 2000). This localization has since been reproduced in human (Mullins et al., 2005), canine (Guziewicz et al., 2007), and mouse (Bakall et al., 2003; Marmorstein et al., 2006) eyes. In a subsequent study (Marmorstein et al., 2002) we used monoclonal antibody clone, E6-1 to perform large scale immunoprecipitation of pBest1 from porcine RPE cells. The specificity of E6-1 and Pab-125 were confirmed using mass spectrometry to identify all of the immunoprecipitated bands that could be isolated from SDS-PAGE gels. In addition to pBest1, only protein phosphatase 2A (PP2A) and HSP-70 were found, and PP2A was determined to interact with Best1 (Marmorstein et al., 2002). We used the combination of Pab-125 and E6-1 or E6-6 to immunoprecipitate and blot back pBest1 from a variety of porcine organ lysates (including kidney, lung, and trachea) and have found that we could identify the protein only in RPE (Stanton et al., 2006) (Fig. 2A).

Studying the expression of Best1 in mouse has been more difficult. Quantitative RT-PCR analysis has revealed a wider distribution of mRNA in mouse than has been observed in man (Kramer et al., 2004), though qRT-PCR baselines are difficult to determine and can vary with the specificity of the primers. Since the C-terminus of mouse and human Best1 are completely divergent the well characterized antibodies (E6-1, E6-6, and Pab-125) described above do not recognize mBest1. We have shown by immunohistochemistry that mBest1 is expressed in the RPE using antibodies raised to the mBest1 C-terminus peptide AESYPYRDEAGTKPVLYE (Pab-003) (Bakall et al., 2003; Marmorstein et al., 2006). Following peptide purification, the Pab-003 antibodies are known to be specific since they do not recognize the RPE of *Best1*$^{-/-}$ mice in immunohistochemical assays (Marmorstein et al., 2006). Similar to the observation by Petrukhin *et al.* (1998)(Petrukhin et al., 1998) that hBest1 is expressed in spinal cord, it has recently been reported that Best1 and Best3 mRNA are expressed in the dorsal root ganglia of the mouse (Al-Jumaily et al., 2007). In dogs, cBest1 mRNA has been detected in RPE and brain by RT-PCR while Northern blot analysis identified Best1 transcripts only in RPE (Guziewicz et al., 2007). All other tissues examined, including testis, kidney, and liver, were negative for cBest1 expression while cBest1 protein was detected by Western blot in RPE. Esumi and co-workers (Esumi et al., 2004) created a transgenic mouse with a *Lac Z* reporter gene under control of the Best1 promoter. Using X-gal staining, they showed that reporter gene expression in the mouse eye is confined to the RPE. They did not, however, examine other tissues, which would help to resolve the controversy regarding extra-ocular expression of Best1 in the mouse.

Whether Best1 is expressed in tissues outside of the eye remains controversial. One study (Duta et al., 2006) used Mab E6-6 to demonstrate expression of hBest1 in human trachea by immunohistochemistry. Barro-Soria *et al.* (2006) report expression of Best1 in human and

mouse airway, colon, and kidney epithelia. However, we have been unable to reproduce these data using antibodies produced in our lab or obtained from commercial sources. Best1 and Best2 expression have also been reported in primary cultures of airway epithelia (Barro Soria *et al.*, 2006; Barro-Soria *et al.*, 2008; Duta *et al.*, 2006; Duta *et al.*, 2004), and both groups have reported that hBest1 is expressed in Calu-3 cells, a cell line derived from human airway epithelia (Barro Soria *et al.*, 2006; Barro-Soria *et al.*, 2008; Duta *et al.*, 2006; Duta *et al.*, 2004). We tested Calu-3 cells obtained from ATCC (Manassas, VA) and grown under similar conditions to those reported by Duta *et al.* (2006) (Fig. 2B-E). Calu-3 lysates were immunoprecipitated with Pab-125 and Best1 in the immunoprecipitates was identified by Western blotting with E6-6 (Fig 2B), E6-1 (Fig. 2C), or a new monoclonal antibody, clone 1C2 [Novus Biologicals (Littleton, CO)] (Fig. 2D). Bands from Calu-3 were compared to bands from positive controls (human RPE, porcine RPE, or fhRPE immunoprecipitates) and negative controls (human cell lines HEK293, MCF-7, rat RPE derived cell line RPE-J). On each blot, a ~70kDa band was identified in the Calu-3 immunoprecipitates. However, this band was present in all immunoprecipitates, including negative controls, and was recognized by all antibodies. In comparison, a slightly lower and stronger band was labeled only in lanes for human and porcine RPE or fhRPE, and co-migrated with recombinant hBest1. These results indicate that the band migrating at ~70kDa is not Best1, and support the conclusion that Calu-3 cells do not produce hBest1. Furthermore, the ~70kDa band was also present in RPE-J cells (Fig. 2E), a rat RPE derived cell line. The C-terminus of hBest1 and rat Best1 (rBest1) differ substantially, and the antibodies that recognize hBest1 are not predicted to recognize rBest1.

The extraocular expression of other bestrophins is less controversial. Best2 expression appears to be more widespread than Best1, albeit at low levels (Bakall *et al.*, 2008; Kramer *et al.*, 2004; Pifferi *et al.*, 2006; Zhang *et al.*, 2008). Studies employing RT-PCR have found Best2 mRNA in eye, colon, nasal epithelium, lung, trachea, salivary glands, and kidney. Using RT-PCR, immunofluorescence staining and Western blotting, Pifferi et al. (2006) reported that Best2 is expressed in nasal epithelia. We recently characterized a *Best2*$^{-/-}$ mouse in which a *Lac Z* gene was inserted in the first two exons of *Best2* placing it under control of the endogenous promoter (Bakall et al., 2008). Using X-gal staining we confirmed expression in eye and colon, but the data were confounded by positive staining in wild type (WT) mice for nasal epithelia. Using an antibody specific for mBest2, we could demonstrate that the protein is expressed in non-pigmented ciliary epithelia (NPE) in the eye, and in colon epithelial cells, but we were unable to confirm expression in nasal epithelia. Since the initial description of the *Best2*$^{-/-}$ mouse, we have also identified Best2 mRNA expression in salivary glands using RT-PCR and the X-gal reporter (our unpublished observations), though we could not detect the protein using immunohistochemistry. Recently Barro-Soria et al. (2008) reported that Best2 is expressed in airway epithelia in the mouse. While we detected mRNA for Best2 in trachea using RT-PCR, this tissue was negative for X-gal staining in *Best2*$^{-/-}$ mice, and did not react with our anti-Best2 antibodies. These data suggest that the positive RT-PCR results may have been due to contamination with salivary gland.

The expression of Best3 and Best4 is broader. In man, RT-PCR studies indicate that Best3 is highly expressed in skeletal and cardiac muscle, testis and thymus (Stohr et al., 2002). RT-PCR studies on mouse tissue find Best3 to exhibit a broader distribution (Kramer et al., 2004). Two groups have reported that full length mouse Best3 mRNA is present in heart (O'Driscoll et al., 2008; Srivastava et al., 2008). Srivastava *et al.* (2008) report that a splice variant containing only exons 2, 3, and 6 is broadly expressed in epithelial organs such as lung, kidney, and salivary glands. As in other studies, the authors did not adequately ensure the specificity of the antibodies used. They did, however, identify bands corresponding to the correct molecular mass for full length mBest3 in heart, and for the shorter splice variant in parotid gland. Best4 mRNA expression is broader including colon, brain, spinal cord, lung,

trachea, and testis (Stohr et al., 2002). No study has addressed Best4 protein expression, and in mice Best4 is an untranscribed pseudogene (Kramer et al., 2004).

3. Bestrophinopathies

Since Frederich Best's report of a hereditary maculopathy in eight members of a family (Best, 1905), his name has been eponymically applied to numerous clinical reports of familial macular disease. Like most autosomal dominant disorders, BVMD has widely varying clinical manifestations. Genomics has allowed us to classify true “Best's disease” as separate from other progressive hereditary maculopathies and pattern dystrophies through identification of mutations in the *BEST1* gene. The clinical features in patients with mutations in *BEST1* seem to cluster into at least four major categories: classical BVMD (OMIM #153700), autosomal dominant vitreoretinochoroidopathy (ADVIRC, OMIM #193220), autosomal recessive bestrophinopathy (ARB, OMIM #611809), and so-called adult-onset vitelliform macular degeneration (AVMD, OMIM #608161). A partial summary of reported mutations in *BEST1* and the diseases they cause is available at the VMD2 mutation database (http://www-huge.uni-regensburg.de/VMD2_database/index.php?select_db=VMD2)

Clinical involvement of abnormalities associated with mutations in *BEST1* is limited to the eye. The primary findings are in the retina but many patients are hyperopic and may have secondary esotropia and various globe deformities. Glaucoma frequently accompanies bestrophinopathies, especially later in life. The major functional impairment, though, is reduced visual acuity, resulting from the macular/retinal disease.

BVMD

Prior to the identification of the *BEST1* gene, a diagnosis of BVMD was based on the presence of a clinically identifiable fundus lesion, family history of the disease, and a sub-normal electrooculogram (EOG) Arden ratio (light peak (LP) / dark trough) with an otherwise normal clinical electroretinogram (ERG) (Cross and Bard, 1974; Marmor, 1979; Mohler and Fine, 1981; Thorburn and Nordstrom, 1978) (Fig. 3). An Arden ratio of 1.5 or lower is typically the threshold for diagnosis of BVMD (Blodi and Stone, 1990; Cross and Bard, 1974), though there have been several cases with Arden ratios >1.5 reported (Caldwell et al., 1999; Wabbels et al., 2006). The low Arden ratio differentiates BVMD from all other bestrophinopathies, other diseases that may present with an apparent vitelliform lesion, and all other inherited maculopathies. Few retinal maladies other than BVMD are associated with a sub-normal EOG Arden Ratio in tandem with a normal ERG, and most are chemical-induced toxicity diseases that preferentially affect the RPE, such as chloroquine retinopathy (Bishara and Matamoros, 1989; Gouras and Gunkel, 1963).

There is a great deal of clinical heterogeneity in classical BVMD as demonstrated by the variability in its presentation and course (Mohler and Fine, 1981). The gross appearance of the fundus among individuals with a subnormal EOG may be completely normal in some patients while in others the macula is severely damaged with gliosis and dense pigmentary scarring (Mohler and Fine, 1981). As a result, the degree of visual impairment varies widely even among patients carrying the same mutation and within the same family (Nordstrom and Thorburn, 1980). Further, vision is often poorly correlated with the appearance of the macula. Even in a group of patients aged 60-84 years mean visual acuity has been reported as 20/40, and acuity is rarely worse than 20/200 to 20/400 (Bard and Cross, 1975; Mohler and Fine, 1981; Renner et al., 2005). The clinical course of BVMD is unpredictable as well. Some 7-9% of individuals with disease causing BEST1 mutations never experience a decrease in acuity (Nordstrom and Thorburn, 1980) while others note episodic vision losses that decrease acuity anywhere between 20/20 and 20/200 (Bard and Cross, 1975; Mohler and Fine, 1981).

Several classification schemes have been proposed to capture the clinical progression of BVMD. We favor that of Mohler and Fine (1981), who delineate at least five major clinical stages of disease based on the appearance of the retinal lesions. These stages do not always occur consecutively nor do they occur inevitably in all patients. Finally, though this scheme is useful in describing the overall spectrum of clinical presentation, it is of limited prognostic value for an individual patient. A significant number of individuals, mostly in the first decades of life, are asymptomatic and have a normal fundus appearance, despite a subnormal EOG light-dark ratio. All of these individuals have stage 0 or pre-vitelliruptive disease. Some of these will never develop clinical disease while others will ultimately have serious macular damage. Predictive criteria for clinical disease progression need to be developed.

Stage I, or pre-vitelliform disease, manifests with only granularity and window defects in the RPE. Stage II is characterized by the presence of a classical vitelliform lesion located in the fovea and can be sub-divided into stages IIa and IIb. Stage IIa is the classical vitelliform “cyst”; a yellow, well-demarcated round lesion that is often compared to the yolk of a “sunny side up” egg in appearance (fig. 4A). In stage IIb (fig. 4B) the borders and yellow color of the lesion become irregular reminiscent of a “scrambled egg”. At stage II, vision is often considerably better than would be expected based on the fundus appearance.

Imaging of stage II lesions using optical coherence tomography reveals what appears to be a well demarcated fluid filled retinal detachment (Pianta et al., 2003; Spaide et al., 2006). The subretinal location of the fluid is also evident from the undisturbed overlying retinal capillary network. Fluorescein angiography and fundus autofluorescence imaging reveals a well demarcated region of autofluorescence within the lesion (Chung and Spaide, 2004; Jarc-Vidmar *et al.*, 2003; von Ruckmann *et al.*, 1997). It is interesting that at this stage elevated autofluorescence does not appear to be panretinal. In rare cases there may be multiple vitelliform lesions scattered at various locations around the retina. Multifocal vitelliform retinopathy is the exception, however, and not the rule in BVMD. Of 16 patients with multifocal vitelliform lesions in 2 separate reports (Boon et al., 2007; Sodi et al., 2007), only 9 carried *BEST1* mutations, those mutations did not differ from those previously reported for classical BVMD, and other family members carrying the same mutations did not present with multiple lesions.

Stage III, or the pseudohypopyon stage (fig. 4C), presents as a partial resorption of the “egg yolk” with reduced vision, sometimes significantly. An apparent fluid line can be visible (fig. 4D) within the lesion, with a window defect due to loss of the RPE above the fluid level while the remaining lipofuscin inferiorly blocks visualization of the choroidal circulation. There is no extravascular leakage of fluorescein unless choroidal neovascularization is present.

The final stage, stage IV, is typically associated with severe vision loss (fig. 4D). Stage IV can be further sub-classified depending on whether the retina is atrophic and hypopigmented (IVa), scarred with fibrous tissue in the macula, often with hyperpigmentation (IVb), or if neovascularization is present beneath and around the gliotic macular scar (IVc). Stage IV carries with it a poor prognosis. Vision at this stage is often <20/100 – 20/200 and does not usually improve.

Although in BVMD there is a general decrease of vision with age, it is noteworthy that about 30% of patients carrying a Best1 mutation retain vision of 20/40 or better into the 5^{th} and 6^{th} decades (Fishman et al., 1993). Among individuals with visible clinical manifestations of the disease at any point in time, 61% have 20/40 or better vision and only 10% are legally blind. In one study of 67 individuals with macular disease, only 1 patient under the age of 46 was legally blind in the better eye (Bard and Cross, 1975). In another group of 91 individuals followed for 8 to 10 years by Mohler and Fine (1981) only 19% lost acuity. Among 47 patients

with a recognizable BVMD phenotype, Fishman *et al.* (1993) found 76% of those under the age of 40 years had an acuity of 20/40 or better. It is interesting to note that visual acuity of individual patients may fluctuate widely over time, independent of age (Fig. 5). This fluctuation is usually associated with Stages II and III (Blodi and Stone, 1990). Among most cases however, the cause of vision fluctuation is not clinically apparent, though some patients anecdotally associate these fluctuations with periods of increased stress and physical activity.

There have been only a handful of reports on the pathology of eyes obtained from donors with BVMD (Frangieh *et al.*, 1982; O'Gorman *et al.*, 1988; Weingeist *et al.*, 1982). Prior to the identification of the *BEST1* gene, O'Gorman et al. (1988) reported a 69 year old donor with stage IVb disease; Frangieh *et al.* (1982) reported an 80 year old stage IV donor. And Weingeist *et al.* (1982) reported on a 28 year old donor with BVMD who had partially resorbed pseudohypopyons (Stage III) in both eyes and visual acuity of 20/30 OD and 20/50 OS. Despite the difference in age and disease state, all three studies found the RPE to be filled with autofluorescent lipofuscin or melano-lipofuscin granules, and that the RPE was relatively intact, despite severe scarring in the 80 year old stage IV donor reported by Frangieh *et al.* (1982).

Since the identification of the BEST1 gene there have been three additional reports on the histopathology of BVMD donor eyes in which the specific mutations underlying the disease were identified (Bakall *et al.*, 2007; Mullins *et al.*, 2007; Mullins *et al.*, 2005). Mullins and co-workers (2005) reported on an 88 year old donor heterozygous for the Y227N mutation in hBest1. The donor had small disciform scars (stage IV) in each macula with visual acuities of 20/30 OD and 20/70+2 OS. The donor exhibited mid-peripheral flecks in the fundus, reminiscent of Stargardt's disease. While the RPE contained substantial lipofuscin, no obvious increase in lipofuscin was noted above that of age-matched donors. Immunoflourescent staining for hBest1 suggested some degree of protein displacement to the apical plasma membrane as well as within the cytosol. In a separate report, Mullins *et al.* (2007) indicate substantial accumulation of lipofuscin granules in the RPE of an 86 year old donor, who was the father of the donor in the study by Weingeist *et al.* (1982) and was determined to be heterozygous for the T6R mutation in hBest1.

Our laboratory reported on the histopathology of an 81 year old donor that was homozygous for the W93C mutation (Bakall et al., 2007). The donor exhibited small disciform scars (stage IV) in both maculae and a visual acuity at age 80 of <20/200 OU. Although the macula contained regions of complete photoreceptor atrophy, a feature also reported by Frangieh *et al.* (1982), the RPE remained intact in much of the macula despite this severe disruption of the neurosensory retina. In a region of the peripheral macula, a large serous detachment of the retina was observed that may represent a stage II vitelliform lesion. Throughout the eye, RPE cells were hypertrophic, positive for PAS, and exhibited substantially elevated autofluorescence due to the accumulation of an excess of intracellular granules. We isolated those granules and compared them to granules isolated from the donor carrying the T6R mutation described by Mullins *et al.* (2005) and to age-matched controls. Granules from the BVMD donors were denser, more autofluorescent, and more numerous. Examination of the isolated granules by electron microscopy indicated a complex multi-lobed structure that differed markedly from controls. Analysis of the A2E content of the granules indicated an overall enrichment of A2E in both BVMD donor eyes relative to age matched controls suggesting that BVMD may share some pathogenic similarity to recessive Stargardt's disease and Stargardt-like macular dystrophy.

In summary, BVMD can be firmly classified as a lipofuscinosis, a disease in which accumulation of lipofuscin is a pathologic characteristic. The origin of this lipofuscin and how it may result in the deterioration of the retina is at present unknown. Although the RPE in

BVMD can contain large numbers of PAS positive, autofluorescent lipofuscin granules, it is important to note that all reports on BVMD donor eye pathology have found the RPE to be generally well preserved despite the accumulation of lipofuscin.

Adult-onset vitelliform macular dystrophy (AVMD)

AVMD shares many clinical similarities with BVMD, though it can also fall into the category of so-called "pattern dystrophies". AVMD frequently occurs sporadically, though it can also be found in autosomal dominant patterns (Zhuk and Edwards, 2006). Histopathologically, AVMD is similar to BVMD in that RPE cells within and around the vitelliform lesion exhibit an increase in autofluorescence and accumulation of lipofuscin granules. Not all cases of AVMD are due to mutations in *BEST1,* as mutations in the *peripherin/RDS* gene have been found in as many as 18% of AVMD / pattern dystrophy patients (Felbor et al., 1997). Clinically, AVMD has traditionally been distinguished from BVMD only by the finding of a normal EOG light-dark ratio (Marmor, 1979). Since genomic studies have only recently been possible, the nosological status of such patients remains unclear. Clinical heterogeneity among patients with mutations in *BEST1* includes a highly variable age of onset. Late onset, even in the 5^{th} and 6^{th} decades for BVMD is not uncommon (Renner et al., 2005). Importantly, although there are several unique *BEST1* mutations associated with AVMD (Allikmets et al., 1999; Kramer et al., 2000), mutations at several sites that cause BVMD also appear to cause AVMD / pattern dystrophy (Allikmets *et al.*, 1999; Kramer *et al.*, 2003; Kramer *et al.*, 2000). A study of 32 unrelated patients with AVMD found four different *BEST1* mutations in eight individuals (Kramer et al., 2000). Two of these mutations were also found in *BEST1* among 34 patients with previously diagnosed BVMD. Such patients likely have BVMD with a late onset of macular disease. Finally, several families with presumptive BVMD have been identified in which the diminished EOG light-dark ratio is progressive, with no defect at early ages (Wabbels et al., 2006). These data suggest that AVMD, when due to a mutation in BEST1, may not be a unique disease, but may simply represent the mildest presentation of BVMD.

Autosomal recessive bestrophinopathy (ARB)

Not all mutant alleles of *BEST1* cause a dominant maculopathy. A recent report (Burgess et al., 2008b) describes seven individuals in five families with irregularities of the RPE throughout the posterior pole with patchy hyperfluoresence on fluorescein angiography, reduced vision (in 6 of 7) and an absent or reduced light rise on EOG in tandem with diminished rod and cone ERGs. All had biallelic mutations in *BEST1* but none of their heterozygous parents who were available for examination had clinical fundus disease, and their EOG and ERG responses were normal. Refractive hyperopia was present in all homozygous individuals and three developed angle closure glaucoma. No vitelliform lesions were observed in any of these patients.

Seven mutational variants in *BEST1* were identified among the affected individuals and all had a variant in both alleles. Among four clinically normal parents who were genotyped, all were heterozygous for a single variant. Further, two affected parents between them had five clinically normal offspring, each of whom inherited one of the variant alleles. Interestingly, three of the variants found have been previously associated with dominantly inherited BVMD. One family has a mutation predicted to result in a premature termination of the protein at Arg200. The authors of the study conclude that ARB probably represents the "null phenotype" for *BEST1* in man (Burgess et al., 2008b).

Autosomal dominant vitreoretinochoroidopathy (ADVIRC)

In 1982, Kaufman *et al.* described a family with a peripheral pigmentary retinopathy, degenerative vitreous changes, and retinal vascular abnormalities which they called autosomal dominant vitreoretinochoroidopathy (ADVIRC) (Kaufman et al., 1982). EOG recordings were not made but similar families reported since then have been found to have a marked reduction

in the EOG LP (Lafaut *et al.*, 2001; Roider *et al.*, 1997; Yardley *et al.*, 2004), ERG abnormalities and mutations in the *BEST1* gene (Burgess *et al.*, 2008a; Yardley *et al.*, 2004). Clinical features of ADVIRC include peripheral chorioretinal atrophy beginning near the equator with a sharp margin and extending to the *ora serrata*, scattered yellowish-white punctate opacities throughout the retina, and retinal neovascularization. The vitreous shows degenerative changes with increased cells, vitreous strands, and often early posterior detachment. Vitreous hemorrhage and cystoid macular edema may occur and are the main causes of decreased vision. Some families have features sometimes seen as part of nanophthalmos, such as hyperopia, microcornea, shallow anterior chambers, and angle closure glaucoma (Lafaut et al., 2001; Yardley et al., 2004).

Two reports on the histopathology of ADVIRC agree that in general, the disease affects primarily the peripheral retina with focal atrophy of the RPE and altered RPE cells surrounding retinal blood vessels and lining the inner limiting membrane (Goldberg et al., 1989; Han et al., 1995). Thus it is dramatically different from the other bestrophinopathies. Since the mutations in *BEST1* associated with ADVIRC are thought to result in exon skipping, understanding how this affects the resultant protein should provide not only clues to the function of Best1, but to the differences in the histopathology of all four bestrophinopathies.

Summary

Mutations in *BEST1* cause 4 clinically distinct human diseases. The differences between the clinical appearance of ADVIRC and ARB from each other, as well as from BVMD and AVMD, are substantial. There is little if any difference however, in the clinical presentation of AVMD due to a *BEST1* mutation and BVMD. Furthermore, the mutation Arg243Val reportedly causes both diseases (Kramer *et al.*, 2003; Kramer *et al.*, 2000). While the diseases are often clinically distinguished purely on the basis of age of onset and family history, a proper diagnosis requires EOG testing. As we were considering the generation of animal models of BVMD, it became apparent that the heterogeneity of the disease could result in difficulties assessing an animal phenotype. Most patients retain significant visual acuity and the disease is often confined to the macula (Bard and Cross, 1975; Blodi and Stone, 1990; Mohler and Fine, 1981). From a histopathologic point of view, the accumulation of lipofuscin and a vitelliform lesion are desirable to recreate, but do not always exhibit a juvenile age of onset, and clinical disease does not occur in up to 9% of patients (Nordstrom and Thorburn, 1980; Renner et al., 2005). Furthermore, the stage II vitelliform lesions typically occur in the fovea, a cone rich region of the retina that is absent from all model organisms that are amenable to genetic manipulation (Marmorstein and Marmorstein, 2007). For this reason, it became apparent that we would need to evaluate RPE function in our animals that corresponds to that assessed clinically using the EOG.

4. The DC-ERG

As noted above, a diagnosis of BVMD has historically been based upon fundus examination and an abnormal EOG LP. Because an abnormal EOG LP in patients with vitelliform lesions is pathognomonic for BVMD, in developing and characterizing rat and mouse models for BVMD, we developed a noninvasive means to record the LP (Peachey et al., 2002; Wu et al., 2004).

In the clinic, the EOG technique used to measure the human LP is based on calibrated eye movements made as the state of retinal adaptation is manipulated in a ganzfeld (Arden et al., 1962; Arden and Kelsey, 1962a; Brown et al., 2006). A similar approach, based on induced eye movements, has been used in sedated animal subjects (Foulds, 1966). Based on these considerations, our first attempt to measure the rat LP was based on EOG recordings made using electrodes placed temporally and nasally while the eye was moved to the left and right

(Peachey et al., 2002). Figure 6 A, and B presents average EOG data obtained using the same stimulus from Sprague-Dawley (A) and Long-Evans (B) rats using induced eye movements, as well as from a normal human subject using calibrated eye movements (Fig. 6C). While the human data includes a distinct large amplitude LP obtained several minutes into the final light adaptation phase, with an Arden ratio of 3.4, the rat data did not include a discernible LP. In fact, compared to the magnitude of the EOG obtained during the dark phase, that measured during the final light phase was unchanged for SD rats (A) and actually lower in LE rats (B). These results indicated that eye movement recordings would not provide a suitable means to measure the LP in animal models of BVMD.

We turned to the dc-ERG, where the LP represents a late component of a complex waveform (Steinberg, 1985; Steinberg *et al.*, 1983) and is present in rodents (Kikawada, 1968). As shown in Figure 7A, the rat dc-ERG includes an initial positive polarity c-wave that follows the b-wave within a few seconds, a negative polarity fast oscillation (FO), and a still later positive polarity LP (Peachey *et al.*, 2002). What is remarkable about these recordings is that the LP levels match well with the EOG data, reaching an asymptote that lies very near the pre-stimulus baseline for Sprague-Dawley rats and just below this level for Long-Evans rats (Peachey et al., 2002). In comparison to the EOG-based approach, the dc-ERG allows the LP waveform to be evaluated for amplitude and kinetic parameters to be measured. As shown in Figure 7B, this conclusion also applies to the mouse, which includes a distinct LP that is somewhat larger than that seen in rats as well as a large amplitude c-wave and FO (Wu *et al.*, 2004).

LP origin

The LP represents a depolarization of the basolateral membrane of the RPE due to activation of a Cl^- conductance (Fujii *et al.*, 1992; Gallemore and Steinberg, 1989, 1993). In contrast to the c-wave and FO, which are triggered by a change $[K^+]$ in the sub-retinal space (Gallemore, 1998), the LP is thought to be triggered by an as yet unidentified "LP substance" secreted by retinal photoreceptors and requiring activation of a second messenger cascade in the RPE (Gallemore, 1998). Changes in either intracellular $[Ca^{2+}]$ or pH were proposed as potential triggers for that conductance. Whether the Cl^- channel(s) that generates this conductance is / are Ca^{2+} sensitive had yet to be determined.

A diminished LP is the hallmark of BVMD. The "CaCC" hypothesis predicts that Best1 generates the LP. To determine the role of bestrophin in generating the LP, we generated and examined *Best1*$^{-/-}$ mice (Marmorstein et al., 2006). Figure 8 shows an example of dc-ERGs obtained from WT, *Best1*$^{-/-}$ and *Best1*$^{-/-}$ mice to a high intensity stimulus. It is clear that all of the major dc-ERG components are present in mice lacking one or both *Best1* alleles. Similar results were obtained at all flash intensities, except at lower stimulus intensities where the LP is somewhat larger in *Best1*$^{-/-}$ mice (Marmorstein et al., 2006). The retention of a LP in mice lacking Best1 is inconsistent with a model of LP generation in which Best1 functions as the primary Cl^- channel underlying this ERG component.

To determine whether there is a role for Ca^{2+} in generating the LP, two approaches were used to manipulate voltage-dependent calcium channels (VDCCs) in rodents. In comparison to vehicle treated animals, rats and mice treated with the VDCC blocker nimodipine exhibited a selective reduction in the LP without a significant alteration of the c-wave or FO (Marmorstein et al., 2006; Rosenthal et al., 2006). To follow up on this observation, we examined mouse mutants lacking different VDCC subunits. The VDCC ion pore is formed by α_1 subunits, but requires β, γ and $\alpha_2\delta$ subunits for normal function (Ball et al., 2003; Khosravani and Zamponi, 2006). To identify the VDCC subunits involved in photoreceptor-to-bipolar cell transmission, we previously surveyed a series of mouse mutants lacking one of the 4 different β subunits, and noted that mice lacking a functional β_2 subunit had normal a-waves but reduced ERG b-waves, indicative of defective synaptic transmission (Ball *et al.*, 2003). When these mice were

tested using the dc-ERG, normal LPs were obtained in animals lacking the β_1, β_2, or β_3 subunits while LPs of *lethargic* mice carrying a naturally occurring null mutation in the β_4 subunit (Burgess et al., 1997) were reduced in amplitude [Fig. 9, (Marmorstein et al., 2006)]. We subsequently noted that comparable LP reductions were present in $Ca_V1.3^{-/-}$ mice lacking the α_{1D} subunit (Wu et al., 2007). While we have yet to identify the γ and $\alpha_2\delta$ subunits that are involved in this process, these results indicate that VDCCs comprised of α_{1D} and β_4 subunits play an important role in LP generation. The finding that Best1 alters the response characteristics of VDCCs (Burgess *et al.*, 2008b; Rosenthal *et al.*, 2006; Yu *et al.*, 2008), and can interact physically with a VDCC β subunit (Yu et al., 2008), suggests that the LP generator is modulated by VDCCs which are in turn modulated by Best1. While we have not as yet identified the Cl^- channel that underlies the generation of the LP, several Cl^- channel mutants have been examined (Wu et al., 2006). Preliminary data indicate that the LP is reduced in mice carrying a single WT allele of *Clcn2* (unpublished) suggesting that this Cl^- channel may play a key role in LP generation.

A final question concerns the manner in which the LP is initiated by the response of the neural retina to light. Although it is possible to evoke a c-wave and FO from an isolated RPE preparation by reducing apical $[K^+]$, it has not been possible to induce a LP *in vitro* (Gallemore, 1998; Steinberg, 1985). This has led to the concept of a *'LP substance'* (*LPS*), a ligand that is required for LP generation and is released by the neural retina to a receptor located on the apical membrane of the RPE. A number of different candidates for the LPS have been examined, including dopamine (Dawis and Niemeyer, 1986; Gallemore and Steinberg, 1990), epinephrine (Joseph and Miller, 1992; Quinn et al., 2001). melatonin (Nao-i et al., 1989) and all-*trans* retinal (Wu et al., 2004). None have received clear support, however. ATP appears to be an attractive candidate for the *LPS*, since it signals through P2 receptors (Brake and Julius, 1996) which are located on the apical RPE membrane (Fries et al., 2004), but this possibility remains to be tested.

Figure 10 summarizes our understanding of the molecules involved in LP generation. While many questions remain, it is clear that LP generation involves the following steps: (1) initiation by light-induced rod photoreceptor activity (Arden and Kelsey, 1962a, b; Wu *et al.*, 2004); (2) alteration of the concentration of an unidentified LPS in the subretinal space; (3) activation of an apical membrane receptor for the LPS ligand; (4) activation of an intracellular signaling cascade which is modified by Best1 and VDCCs; (5) activation of a basal membrane Cl^- channel, ultimately depolarizing the basal membrane of RPE cells.

5. Animal Models of Bestrophinopathies

Since the identification by Keeler in 1924 (Keeler, 1924) of the rodless mouse model, the first recognized spontaneous mouse model of photoreceptor degeneration, the mouse has become the principle model organism for the study of this broad class of diseases (Chang et al., 2002). The ability to manipulate the mouse genome has resulted in a surge in the use of mice to model retinal degenerative diseases. Mouse models recapitulating the major symptoms of retinal disorders such as retinitis pigmentosa, cone-rod dystrophies, and Leber's congenital amaurosis have now been created, resulting in a profound increase in our understanding of these and related diseases as well as providing a testing platform for various therapeutic interventions (Dalke and Graw, 2005; Pacione *et al.*, 2003). The mouse retina is composed predominantly of rod photoreceptors with cones accounting for only 2-3% of the total photoreceptor population (Carter-Dawson and LaVail, 1979; Szel et al., 1996). The mouse retina is, for this reason, structurally more akin to the peripheral retina than the macula of humans. Unfortunately, no organism that is amenable to genetic manipulation has an anatomic macula (Marmorstein and Marmorstein, 2007). From the point of view of studying the bestrophinopathies, this is acceptable. For example, significant insights into the function of the

genes ABCA4 and ELOVL4, both causing macular degenerations characterized by accumulation of lipofuscin in the RPE, have been provided by mouse models despite the lack of a perfect recapitulation of the key disease feature of a degenerating macula (Agbaga *et al.*, 2008; Karan *et al.*, 2005; Radu *et al.*, 2004; Radu *et al.*, 2008; Vasireddy *et al.*, 2006; Vasireddy *et al.*, 2007; Weng *et al.*, 1999). That the EOG LP is altered in BVMD clearly indicates that this RPE defect is not restricted to the macula, but is instead a panretinal abnormality of RPE function that should manifest in the mouse as a change in the LP of the dc-ERG. This position is supported by the most common histopathologic finding in BVMD eye donors of an accumulation of lipofuscin throughout the retina (Bakall *et al.*, 2007; Frangieh *et al.*, 1982; Mullins *et al.*, 2007; Mullins *et al.*, 2005; O'Gorman *et al.*, 1988; Weingeist *et al.*, 1982). In comparison, the mouse may not be a good model for the vitelliform lesion, which is restricted to the macula and in the overwhelming majority of cases involves the fovea. That ganzfeld ERG and EOG changes are noted in patients with ADVIRC or ARB also indicates that these are panretinal diseases, despite a distinct macular defect. Thus, it is reasonable to attempt modeling of the bestrophinopathies in the mouse, with the expectation that the disease phenotype will be restricted to abnormalities that affect the human peripheral retina (i.e., changes in RPE electrical function as measured by the dc-ERG and an age-related accumulation of lipofuscin).

Rat models of BVMD

As stated earlier, we initially developed techniques to record dc-ERGs from rats because they were larger in size and we initially focused on adenovirus-mediated transfection of the RPE with BVMD associated hBest1 mutants. When injected subretinally, both W93C and R218C mutant hBest1 protein were expressed and properly transported to the rat RPE basolateral plasma membrane (Marmorstein et al., 2004). These observations indicate that protein trafficking defects do not underlie the pathogenesis of BVMD due to these 2 mutations. Although the ERG a- and b-waves were diminished due to surgery, the differences were similar regardless of whether the eye received an empty vector (control), WT hBest1, or mutant hBest1 (Marmorstein et al., 2003; Marmorstein et al., 2004).

There were distinct effects of WT and mutant hBest1 over-expression on the components of the dc-ERG. For all constructs, the effects on the c-wave and FO were marginal and varied with the dose of the adenoviral vector. While the CaCC hypothesis predicted that over-expression of WT hBest1 would dramatically increase the amplitude of the LP component, any increase was modest and was not clearly related to the level of hBest1 over-expression (Fig 11). In comparison, transfection with mutant (W93C or R218C) hBest1 resulted in a decrease in LP amplitude and a rightward (desensitizing) shift of the LP luminance-response function (Fig. 11). These data were the first indication that the LP may not be simply generated by Best1. However, the diminished LPs observed in response to the expression of mutant hBest1 were consistent with a dominant negative effect as predicted by the CaCC hypothesis.

Mouse models of BVMD

Having established the utility of the dc-ERG in analyzing Best1 induced effects on the LP of the rat, we next moved to the development and evaluation of mouse models. The CaCC hypothesis dictates that the complete absence of Best1 CaCC activity should be the most extreme manifestation of BVMD, and so we generated *Best1*$^{-/-}$ mice lacking the m*Best1* gene as well as “knock-in” mice whose endogenous m*Best1* alleles were altered to carry BVMD causing mutations. These mouse models differ substantially from the rat model since Best1 expression would be at normal endogenous levels or absent, rather than being overexpressed, and there would be no potential for cross-species incompatability (we used hBest1 in the rat studies). Finally, we could examine the impact of bestrophin mutations on the retina and RPE in the absence of a background level of WT mBest1 expression. In these models, we could test

directly several specific predictions of the CaCC hypothesis: that the LP should be dramatically reduced In *Best1*$^{-/-}$ mice, that LP abnormalities should be observed in knock-in mice expressing mutant forms of mBest1 and that these abnormalities should be more severe in mice expressing two rather than one knock-in alleles.

Best1$^{-/-}$ mice were viable and exhibited no outward signs of disease, and the absence of mBest1 expression was verified at both the mRNA and protein levels (Marmorstein et al., 2006). No histological evidence of photoreceptor loss in *Best1*$^{-/-}$ mice up to 14 months of age and ERG a- and b-waves were comparable to those of *Best1*$^{+/+}$ littermates. The c-wave and FO components of Best1$^{-/-}$ mice were indistinguishable from those of WT littermates at all stimulus intensities examined. Although the CaCC hypothesis dictates that the LP should be markedly reduced or abolished in *Best1*$^{-/-}$ mice, LPs obtained to high intensity stimuli were comparable to those of WT littermates (Fig. 8) while LPs obtained to low intensity stimuli were actually larger in *Best1*$^{-/-}$ mice than in WT littermates. Based on these data it can be concluded that mBest1 is not necessary to generate the mouse dc-ERG LP.

We also generated a knock-in mouse line carrying the BVMD-associated W93C mutation in *mBest1* (Stanton, 2008). ERG a- and b- waves of W93C knock-in mutants are similar to those of WT littermates. However, consistent with the LP deficits in BVMD patients, dc-ERG recordings revealed significant differences in the LP component amongst Best1^{W93C} genotypes. Compared to WT littermates, the LP responses of *Best1*$^{+/W93C}$ and *Best1*$^{W93C/W93C}$ mice were enhanced at low stimulus intensities, and were reduced in the middle of the intensity range (Fig. 12). As a result, there was little modulation of LP amplitude between -1.0 and +1.0 log cd/m^2, where the WT response demonstrates a marked increase. In this intensity range, the results of *Best1*$^{+/W93C}$ and *Best1*$^{W93C/W93C}$ mice also differ from those of *Best1*$^{-/-}$ mice, whose LP response is also consistently greater than that of WT mice but is modulated by stimulus intensity. Neither *Best1*$^{+/W93C}$ mice nor *Best1*$^{W93C/W93C}$ mice exhibited a maximum LP amplitude that was significantly different from their WT littermates. We conclude from these data that *Best1*$^{+/W93C}$ and *Best1*$^{W93C/W93C}$ reproduce the sole fully penetrant symptom of BVMD and that the diminished LP in human BVMD patients, at least in early phases of the disease, is most likely due to a shift in the luminance-response function, a feature of the EOG that is not routinely examined (Brown et al., 2006).

Histopathologic analysis of *Best1*$^{+/W93C}$ and *Best1*$^{W93C/W93C}$ mice up to 24 months of age revealed a substantial accumulation of lipofuscin compared to age-matched WT littermates (our unpublished observations), indicating that the mice replicate a second aspect of human BVMD, namely the accumulation of lipofuscin in their RPE cells. Even at 2 years of age, the RPE was generally intact, although regions of RPE hypertrophy were noted, especially adjacent to the optic nerve head. These findings are very similar to what has been observed in human donor eyes from a BVMD patient carrying the W93C mutation (Bakall et al., 2007).

Most recently, we examined a second knock-in for the BVMD-associated R218C mutation. ERG a- and b-waves of *Best1*$^{+/R218C}$ and *Best1*$^{R218C/R218C}$ mice are comparable to those of WT littermates, and our initial examination of *Best1*^{R218C} mice reveals a dc-ERG phenotype similar to the Best1^{W93C} mice. Further analysis of these mice is an active pursuit of our laboratories.

Canine model

Mutations in canine Best 1 (cBest1) have been identified in a naturally occurring retinal disorder termed *canine multifocal retinopathy* (*cmr*) (Guziewicz et al., 2007). These mutations have been described in Great Pyrennes, Coton de Tulear, English Mastiff, and Bullmastiff breeds, and may reflect the common ancestries of these breeds. In all cases *cmr* is inherited as an autosomal recessive trait, and was initially identified and mapped based on the presence of

multiple vitelliform like lesions, RPE hypertrophy, and enhanced RPE autofluorescence. Guziewicz et al. (2007) found mutations in cBest1 in affected animals from two lines of *cmr*: R25X (*cmr1*) and G161D (*cmr2*). The R25X mutation is predicted to result in a null phenotype, though it is possible that initiation could occur at Met52 resulting in a cBest1 protein lacking TM1. Perhaps reflecting the difficulty of working a larger animal model with a relatively slow breeding cycle, experiments have not yet been published to distinguish these two possibilities.

The pathophysiology of *cmr* is similar to multifocal vitelliform dystrophy (MVD). Although MVD in the human population is rare, >50% of human MVD cases examined have mutations in one allele of *BEST1* (Boon et al., 2007). No individual homozygous for BEST1 mutations has been reported with MVD (Bakall *et al.*, 2007; Burgess *et al.*, 2008b; Nordstrom and Thorburn, 1980). It is interesting to note that heterozygous carriers of *cmr*-associated cBest1 mutations do not exhibit clinical disease, though the electrophysiological characteristics (EOG, ERG) of *cmr* have not yet been reported and may reveal the carrier state. Although *cmr* exhibits some pathologic similarities to BVMD, the recessive pattern of inheritance and potential null phenotype indicate that *cmr* is more akin to ARB. However, the presentation of *cmr* differs substantially from ARB, which does not present with vitelliform lesions. Further study is required to understand how this canine model relates to human bestrophinopathies.

Bestrophin-2 mouse model

The phenotype of the *Best1*$^{-/-}$ mouse indicated that Best1 is not necessary to generate the LP. However, early studies on the expression of Best2 suggested that it is also expressed in RPE cells (Kramer et al., 2004) suggesting the possibility that Best2 may compensate for the absence of Best1. To address this, we characterized a *Best2*$^{-/-}$ mouse line (Bakall et al., 2008; Zhang et al., 2008). Similar to Best1, *Best2*$^{-/-}$ mice are healthy and do not exhibit a retinal degeneration phenotype. In the *Best2*$^{-/-}$ mouse, the *Lac Z* gene was inserted into the *Best2* gene, placing it under control of the endogenous *Best2* promoter and providing a means to analyze *Best2* tissue expression. In *Best2*$^{-/-}$ and *Best2*$^{+/-}$ mice, only colon, salivary gland, and eye were consistently and strongly positive for X-gal staining. As noted above, prior reports indicated that Best2 is expressed in airway and nasal epithelia (Barro-Soria *et al.*, 2008; Pifferi *et al.*, 2006). Although nasal epithelia were positive for X-gal staining, this was only apparent with prolonged incubation times. Moreover, in every instance, the nasal tissues from WT control mice (not expressing X-gal)) were positive as well. Lung, trachea, hind brain, and skeletal muscle, all positive by RT-PCR, were negative for X-gal staining. In the eye, we were surprised to find that X-gal staining was confined to non-pigmented epithelial (NPE) cells rather than the RPE as anticipated. No X-gal staining was observed in other ocular tissues. The expression of Best2 was confirmed in NPE and colon by immunofluorescence staining with an antibody specific to mBest2 (Fig 13A) but not in any other tissue tested.

We also examined Best2 expression in human eyes using RT-PCR of total RNA isolated from RPE or ciliary body. In the human eye, the expression pattern is the same as that observed in mouse (Bakall et al., 2008), a finding that we have now confirmed by immunoprecipitation of Best2 from human ciliary body, and immunofluorescence staining of NPE cells in human donor eyes (our unpublished results).

We have crossed *Best1*$^{-/-}$ and *Best2*$^{-/-}$ mice to create double knock-outs. *Best1*$^{-/-}$/*Best2*$^{-/-}$ mice do not develop a retinal degeneration phenotype or a LP deficit (our unpublished observations). The presence of Best2 in NPE cells suggested a role in the generation of aqueous humor, which relies on a Cl^- conductance to transport fluid from the stroma into the anterior chamber of the eye. *Best2*$^{-/-}$ mice were found to exhibit a lower intra-ocular pressure (IOP) than *Best2*$^{+/+}$ mice (10.22 ± 0.16 vs 11.70 ± 0.16 mm Hg; see Fig. 13B), a significant ($P < 0.0001$) difference of 1.48 mm Hg. After accounting for episcleral venous pressure (6.3 mm Hg in both *Best2*$^{+/+}$ and *Best2*$^{-/-}$ mice) we find that disruption of Best2 results in a 27% decrease in IOP. However a

comprehensive study of aqueous dynamics in these mice demonstrated that aqueous flow was increased by 73% in Best2$^{-/-}$ mice and that this was compensated for by enhanced drainage. We concluded from this study that Best2 is an antagonist of aqueous flow, not one of the Cl^- channels that generate it (Zhang et al., 2008).

6. The Function of Best1

Are bestrophins CaCCs?

The hypothesis that Best1 is a CaCC originated from the following observations: (*i*) individuals with BVMD, at the time the only disease known to be caused by *BEST1* mutations, have a diminished EOG LP; (*ii*) the LP was known to be generated by a Cl^- conductance across the basolateral membrane of the RPE; (*iii*) that Cl^- conductance was postulated to be Ca^{2+} sensitive; (*iv*) Best1 is localized to the basolateral membrane of the RPE cell. Sun *et al.* (2002) produced three lines of experimental evidence to support this hypothesis. The first was the identification of hBest1 tetramers or pentamers, a structure that would support the formation of a channel pore. The second was the induction of CaCC conductances in HEK293 cells by transfection with hBest1 and other bestrophin family members. The third was the absence of CaCC activity in HEK293 cells transfected with BVMD-associated hBest1 mutants, and an apparent dominant negative effect of these mutants on WT Best1 activity. Based on these observations, Sun *et al.* (2002) proposed the "CaCC hypothesis" which states that Best1 is the CaCC responsible for generating the LP, and that BVMD is caused by a loss of Best1 CaCC activity due to a dominant negative effect.

A series of clinical and laboratory observations, accumulated during the last 6 years, cast these observations in a different light and support a competing hypothesis for Best1 function. As noted above, *BEST1* mutations are now associated with four distinct human retinal diseases, one of which, ARB, exhibits recessive inheritance (Burgess et al., 2008b). ARB has a distinct clinical presentation from that of BVMD, AVMD, and ADVIRC. If BVMD and AVMD are due to loss of CaCC activity, then ARB, if a true null phenotype, would be predicted to resemble BVMD and AVMD, although perhaps with greater severity. Contrary to this prediction, ARB shares little clinical similarity with BVMD or AVMD. Furthermore, missense mutations associated with ARB do not exhibit Cl^- channel activity, and do not exhibit dominant effects on WT hBest1 (Burgess et al., 2008b). This point is important because it is also true of the *BEST1* mutation A243V which causes AVMD (Yu et al., 2006). Since AVMD and ARB exhibit dramatically different clinical presentations, both cannot be due simply to loss of Best1 activity. If ARB results from a true Best1 null phenotype then the differences between ARB and AVMD/BVMD also indicate that AVMD/BVMD are unlikely to be due to a loss of Best1 CaCC activity. Therefore, the dominantly inherited bestrophinopathies must be due to Best1 dysfunction rather than absence of Best1 function.

Further evidence against the CaCC hypothesis has been obtained in the study of animal models. We isolated RPE cells from *Best1*$^{-/-}$ mice and examined CaCC conductances using whole cell patch clamp (Marmorstein et al., 2006). No differences were noted between cells isolated from *Best1*$^{-/-}$ mice or WT littermates, indicating that any mBest1-associated Cl^- conductance plays only a minor role in the total Cl^- conductance of the RPE cell. Perhaps the most compelling experimental observation is that *Best1*$^{-/-}$ mice continue to generate a clear LP that which is actually larger in amplitude than that obtained from WT mice under certain stimulus conditions (Marmorstein et al., 2006). *Best1*$^{-/-}$ mice also develop no obvious retinal defects, and do not exhibit abnormal lipofuscin accumulation, even at very old ages (our unpublished observations). These observations contrast with results obtained in *Best1*^{W93C} mice, which exhibit an altered dc-ERG response that includes a diminished LP at stimulus luminance levels similar to that used in human EOG testing (Stanton, 2008) and an age-related accumulation of lipofuscin (our unpublished observations), reminiscent of the primary histopathological

findings in BVMD. These mouse results indicate that it is very unlikely that the W93C mutation inactivates Best1 function. On the other hand, the canine *cmr* models suggests that a null phenotype would produce MVD (Guziewicz et al., 2007). The rare instance of multifocal Best disease in man, however, is associated with a dominant mode of inheritance and occurs sporadically in families with an otherwise normal etiology (Boon et al., 2007; Sodi et al., 2007). Canine *cmr* appears to differ clinically from ARB and ADVIRC as well, suggesting that there may be additional modifier genes, or physiologic features that underlie the unique *cmr* phenotype. Although there is as yet no report on the electrophysiology of *cmr*, there appears to be little consistency between putative null phenotypes, and none of the putative null conditions described in mouse, dog, or human are consistent with the diagnosis of AVMD/BVMD. We believe that this evidence rules out the hypothesis that loss of Best1 function causes BVMD.

The CaCC model of Best1 argues that Best1 is an essential CaCC required to generate the EOG LP. Although the EOG Arden ratio is normally affected in BVMD, there are exceptions to this rule, and by definition there is no reduction in the EOG LP in AVMD. While both ADVIRC and ARB patients exhibit diminished EOGs, diminished ERGs indicate that these may reflect reduced retinal activity driving the RPE response (Won et al., 2008). *Best1*$^{-/-}$ mice, exhibit a normal or enhanced LP, while other models or manipulations act to reduce LP amplitude (Wu et al., 2006). From these results, we conclude that Best1 is not required to generate the LP, but in fact serves to antagonize it.

A second argument to support the CaCC hypothesis was the finding that Best1 forms tetramers or pentamers. That level of oligomerization would be sufficient to provide a minimum of 16 membrane spanning domains, enough to form a channel pore (Sun *et al.*, 2002(Stanton et al., 2006). However, we have found that pBest1 extracted from tissue forms homodimers (Stanton et al., 2006). While it is true that the dimers may interact to form higher ordered multimers, there is currently no experimental evidence to demonstrate that this occurs in tissue. The larger oligomers formed in HEK293 cells likely result from aggregation of overexpressed protein (Stanton et al., 2006). As a consequence, there is insufficient data to indicate that the quaternary structure of Best1 required to form a pore actually occurs in nature, a key feature supporting the CaCC hypothesis.

Perhaps the most compelling evidence for Best1 CaCC function are the heterologous expression studies in HEK293 cells. Based on results reported by many laboratories, it is now clear that expression of any bestrophin is capable of inducing a voltage dependant anion conductance. But does this conductance represent a CaCC and are the currents carried by bestrophin channels? The strongest evidence for this is that mutation of specific amino acids in the second transmembrane domain of Best2 alters ion selectivity (Qu *et al.*, 2006; Qu *et al.*, 2004; Qu and Hartzell, 2004). However, hBest1 and mBest2 have a 10-times higher affinity for Ca^{2+} than do classical CaCCs and, in general, bestrophins do not exhibit the same voltage-dependent kinetics and outward rectification as classical CaCCs (Qu *et al.*, 2004; Qu *et al.*, 2003; Sun *et al.*, 2002). Furthermore, classical CaCCs exhibit voltage dependent kinetics and outward rectification that is not seen with hBest1. Finally, heterologously-expressed bestrophins have never been shown to be activated by receptors that elevate cytosolic Ca^{2+} such as those for the candidate LPS (e.g. ATP, epinephrine, and dopamine). Still, Xiao and co-workers (Xiao et al., 2008) have recently demonstrated that Best1 binds Ca^{2+} to an EF1 domain. Mutations in this domain affect channel gating and several disease associated mutations have been described in this domain.

In contrast to the bestrophins, three groups have independently demonstrated that TMEM16A/ano1 functions as a CaCC (Caputo et al., 2008; Schroeder et al., 2008; Yang et al., 2008). These reports included unambiguous single channel recordings. Each group used RNA interference

(RNAi) to reduce the expression of TMEM16A/ano1 in various mammalian cells and tissues and in each case RNAi treatment disrupted cellular processes that one would expect to be disrupted following reduced expression of CaCCs. The phenotype of the TMEM16A/ano1 knock-out mouse is neonatal lethal due to tracheomalacia (Rock et al., 2008). The protein is expressed in airway epithelia and appears to be responsible for the CaCC activity of that tissue. Furthermore, over-expression of TMEM16A/ano1 induces an ionic current with the properties expected of a CaCC expressed in a heterologous system. The structure of the protein is similar to that of other channel proteins, in contrast to the bestrophins, and the introduction of mutations at critical sites in the TMEM16A/ano1 alter channel function. Finally, TMEM16A/ano1 can be activated in cells by receptors at the cell surface that, when activated themselves, cause release of intracellular Ca^{2+} stores.

Few studies have been carried out on bestrophins in native cells that are known to express the proteins. In *Best1*$^{-/-}$ and *Best2*$^{-/-}$ mice the absence of these bestrophins does not correlate with a deficit in CaCC activity in the RPE (Marmorstein et al., 2006), or in salivary acinar cells (James Melvin, University of Rochester, personal communication). Duta *et al.* (2004, 2006) and Barro-Soria *et al.* (2006, 2008) have characterized bestrophins in airway epithelia. However, it now appears that TMEM16A/ano1 is responsible for CaCC conductances in airway epithelia (Yang et al., 2008). In contrast to the severe phenotype of the TMEM16A/ano1 knock-out mouse (Rock et al., 2008), *Best1*$^{-/-}$ mice exhibit no obvious systemic defects (Barro-Soria *et al.*, 2008; Marmorstein *et al.*, 2006). This also implies that Best1 may not be responsible for CaCC conductances in airway epithelia.

We have sought to study the role of hBest1 in the only cell type definitively shown to produce the protein, the RPE. In contrast to RPE derived cell lines, which produce hBest1 mRNA, but not protein (Marmorstein et al., 2000) primary cultures of hfRPE do express hBest1 protein (Hu and Bok, 2001; Maminishkis et al., 2006), although maximum expression in our experience does not develop until 4-8 weeks in culture. Using these cells, we have observed an increase in I_{sc} due to hBest1 over-expression. That increase is mediated primarily by an increased transepithelial Cl^- conductance. However, despite a clear increase in the amount of hBest1 expressed, the polarity of the protein is not altered, and the amount of hBest1 detected at the cell surface is not increased beyond that observed due to endogenous expression (our unpublished observations). Nevertheless, more Best1 should be at the cell surface if it is responsible for the increased contribution of Cl^- transport to the I_{sc}. When those same monolayers are stimulated with ionomycin, we see no increase in I_{sc} in fhRPE monolayers above that observed in control monolayers, and the CaCC inhibitor niflumic acid returns I_{sc} to similar levels in control and hBest1 overexpressing monolayers (our unpublished observations). A conclusive demonstration that hBest1 is a CaCC would require either single channel recordings that could be unambiguously attributed to a bestrophin, or the observation of CaCC activity associated with recombinant bestrophin in planar lipid bilayers. To date, there is only one report describing *drosophila* bestrophin associated single channel recordings (Chien et al., 2006). These currents were small, and required ATP, a unique property not associated with bestrophin channel activity recorded under whole cell patch clamp (Hartzell et al., 2008a).

Bestrophins as regulators of ion transport and homeostasis

There is a great deal of evidence supporting the idea that bestrophins are CaCCs or at the least, Ca^{2+} dependent anion channels when expressed in heterologous systems. There is also a growing body of evidence, derived from the human disease state and studies in animal models that suggests, at least for Best1 and Best2, that their primary role *in situ* is not that of ion channel but of channel regulator.

Since we had established that the LP luminance response is altered in mice lacking VDCC subunits (Marmorstein et al., 2006; Wu et al., 2007), we examined changes in $[Ca^{2+}]i$ in *Best1*$^{-/-}$ mice stimulated with extracellular ATP, a candidate LPS. The increase in $[Ca^{2+}]i$ stimulated by ATP was approximately 7-fold greater in *Best1*$^{-/-}$ mice than in *Best1*$^{+/+}$ littermates (Marmorstein et al., 2006) (Fig. 14). Conversely, we find that the increase in $[Ca^{2+}]i$ stimulated by ATP in knock-in mice carrying the W93C mutation in Best1 is suppressed (our unpublished observations). These results indicate that Best1 may function to antagonize the LP through specific effects on Ca^{2+} signaling. When expressed heterologously, Best1 alters the response kinetics of VDCCs, accelerating channel opening and closing (Burgess *et al.*, 2008b; Rosenthal *et al.*, 2006; Yu *et al.*, 2008). The Best1 mutants W93C and R218C appear to affect the kinetics differently: W93C slowed activation and inactivation, while R218C accelerated activation and inactivation (Rosenthal et al., 2006; Strauss, 2008). Yu et al. (2008) have recently shown that Best1 can interact physically with the VDCC β_3 subunit via its cytosolic domain, a finding recently confirmed by Strauss and co-workers (Strauss, 2008).

To further investigate the effects of Best1 on Ca^{2+} signaling we examined the response of fhRPE monolayers to extracellular ATP. ATP has been shown to induce a rapid increase in the TEP of fhRPE monolayers (Peterson et al., 1997). Monolayers overexpressing Best1^{W93C} exhibit a smaller response to ATP than controls. Measurement of $[Ca^{2+}]i$ using the Ca^{2+} indicator dye fura-2 demonstrated that cells overexpressing Best1^{W93C} have a slower and more shallow increase in $[Ca^{2+}]i$ than either control cells or Best1 overexpressors. Washout of ATP, which caused a rapid reduction in $[Ca^{2+}]i$ in control cells did not result in a return to baseline $[Ca^{2+}]i$ in Best1^{W93C} expressing cells. It should also be noted that on average, resting $[Ca^{2+}]i$ was Best1-dependent, with Best1 overexpressors exhibiting lower and Best1^{W93C} cells exhibiting higher values than controls (our unpublished observations).

We have gained additional insights from the Best2$^{-/-}$ mouse. IOP was lowered to a greater extent in *Best2*$^{+/-}$ and *Best2*$^{-/-}$ mice by the carbonic anhydrase (CA) inhibitor dorzolamide than in WT littermates (Bakall et al., 2008). CA catalyzes the reversible hydration of CO_2 according to the reaction:

$$H^+ + HCO_3^+ \overset{CA}{\leftrightarrow} H_2CO_3 \leftrightarrow CO_2 + H_2O$$

CO_2/HCO_3^+ is the primary pH buffering system in cells. Recently Qu and Hartzell (2008) reported that bestrophins conduct HCO_3^- equal to or better than Cl^-(Qu and Hartzell, 2008). While this remains to be confirmed, these data suggest a role for bestrophins in regulation of intracellular pH if not directly in HCO_3^- transport, and suggest an additional means by which they may participate in RPE fluid transport. There is a critical relationship between pHi and $[Ca^{2+}]i$ that is well illustrated by the ischemia reperfusion injuries that occur acutely in heart attacks and stroke (Allen *et al.*, 1993; Allen *et al.*, 1989; Elliott *et al.*, 1992; Lee and Allen, 1992; Piper *et al.*, 1996; Piper *et al.*, 2003; Xiao and Allen, 2000; Yao and Haddad, 2004; Zhou *et al.*, 2004). In both instances increases in $[Ca^{2+}]i$ occur when cells acidify in response to a buildup of CO_2. Photoreceptors have higher rates of oxygen consumption of any cell (Birol *et al.*, 2007; Haugh *et al.*, 1990; Wangsa-Wirawan and Linsenmeier, 2003) resulting in the production of large quantities of CO_2 and H_2O as byproducts of respiration. Photoreceptor respiration is light sensitive (Birol *et al.*, 2007; Haugh *et al.*, 1990). Failure to compensate for changes in CO_2 and H_2O production by the photoreceptors would result in acidification of the sub-retinal space, similar to what occurs during ischemia, and this could lead to abnormalities including serous retinal detachments. RPE fluid transport is governed at least in part by mechanisms that are Ca^{2+} sensitive. Studies on cardiac and neuronal ischemia teach us that

intracellular [Ca^{2+}] and pH are intimately related to each other and to local concentrations of CO_2/HCO_3 (Allen *et al.*, 1993; Allen and Xiao, 2003; Lang *et al.*, 2003; Park *et al.*, 1999; Piper *et al.*, 1996; Piper *et al.*, 2003; Xiao and Allen, 1999, 2000; Yao *et al.*, 2003; Yao and Haddad, 2004). In fact, VDCC inhibitors such as nimodipine are given to stroke victims to prevent cell death following ischemia (Abernethy and Schwartz, 1999). Another strategy for protection from ischemic injury that is currently undergoing clinical trials is inhibition of Na^+/H^+ exchange (NHE) (Karmazyn et al., 2001; Mentzer et al., 2008). NHE inhibitors are protective against ischemic injury in animal models (Karmazyn et al., 2001; Masuoka et al., 2005; ten Hove et al., 2007), and the NHE1 knock-out mouse is resistant to ischemic damage (Luo *et al.*, 2005; Wang *et al.*, 2003). Interestingly, in a recent study, dBest1 expression was down-regulated in *drosophila* strains adapted to a low O_2 environment (Zhou et al., 2007). Although it was not clear from that study what the role of dBest1 is in adapting to those conditions, as stated above, we have recently found that Best1 is a potent regulator of Ca^{2+} signaling and a HCO_3^- dependent, regulator of Na^+/H^+ exchange (our unpublished observations).

7. Conclusions: A New Hypothesis to Explain the Etiology of Bestrophinopathies

There is a great deal of data regarding the function of the bestrophin family of proteins. Although it is now clear that the CaCC hypothesis has failed multiple tests, the key question of how Best1 mutations cause four distinct retinal degenerative diseases remains. The pathogenesis of the bestrophinopathies is not the result of the diminished LP; the formation of a vitelliform lesion and accumulation of lipofuscin occur not only in BVMD, but in AVMD which by definition has a normal Arden ratio. A major problem with the CaCC hypothesis of Best1 function was that it failed to offer an explanation for the accumulation of lipofuscin that characterizes the bestrophinopathies. Any new hypothesis of Best1 function must satisfactorily explain not only the LP deficit in BVMD, but the accumulation of lipofuscin, and the formation of vitelliform lesions in AVMD / BVMD, diffuse fluid filled retinal detachments in ARB, and the peripheral retinopathy in ADVIRC. Recent data point to a role for the bestrophins in regulating intracellular [Ca^{2+}] (Burgess *et al.*, 2008b; Marmorstein *et al.*, 2006; Rosenthal *et al.*, 2006; Yu *et al.*, 2008) and pH (our unpublished observations) (Fig. 15A). Effects of Best1 on VDCCs (Fig. 15A, 1) are now well documented (Burgess *et al.*, 2008b; Rosenthal *et al.*, 2006; Yu *et al.*, 2008) and indicate what is most likely an antagonistic role. Data from the $Best1^{-/-}$ and $Best1^{W93C}$ mice suggest that Best1 can inhibit release of Ca^{2+} stores following stimulation with ATP (Fig 14 & Fig. 15A, 2, 3) (Marmorstein et al., 2006; Stanton, 2008). Finally, it appears that Best1 plays a role in regulation of pH via both HCO_3^- transport (Qu and Hartzell, 2008) and modulation of NHE activity (Stanton, 2008) (Fig. 15A, 4). It should be noted that in the first description of Bestrophin associated channel activity (Sun et al., 2002), it was hypothesized that Best1 may function as a general anion or HCO_3^- channel. While the majority of subsequent work has focused on the possible CaCC activity of the bestrophins, the finding that Best1 efficiently transports HCO_3^- (Qu and Hartzell, 2008) combined with our findings in knock-in and knock-out mice cause us to believe that future studies of Best1 channel activity should focus on HCO_3^- rather than Cl^-.

So what can we hypothesize about the role of Best1 in a healthy RPE cell? As Fig. 15A illustrates, we suggest that Best1 plays a role in intracellular Ca^{2+} and pH homeostasis. Specifically we suggest that Best1 may function to set gain on changes in intracellular Ca^{2+} that result from G-protein coupled receptor (GPCR) signaling, and that it functions to modulate the setpoint of NHE in response to HCO_3^- levels in the RPE cell. The by-products of photoreceptor respiration H_2O and CO_2 must be transported from the sub-retinal space to the choroidal circulation. This is a job performed by the RPE. The level of oxygen utilization by photoreceptors varies with light / dark level and as such so does the production of respiratory

waste products (Birol *et al.*, 2007;Wangsa-Wirawan and Linsenmeier, 2003). We suggest that Best1 serves to set the gain of those systems in the RPE that must respond to changes in the volume of photoreceptor waste products, which otherwise would cause cell / tissue volume and pH changes. RPE H_2O transport is regulated by GPCR signaling involving Ca^{2+}; RPE pH must remain stable despite changes in intracellular [HCO_3^-] resulting from CO_2/HCO_3^- transport.

How then does dysfunction of Best1 rather than a loss of function result in BVMD or another bestrophinopathy? Both Ca^{2+} and pH play important roles in RPE phagocytosis (Deguchi *et al.*, 1994; Feeney-Burns and Eldred, 1983; Hall *et al.*, 1991; Kaemmerer *et al.*, 2007; Karl *et al.*, 2008; Kim *et al.*, 2006; Liu *et al.*, 2008; Peters *et al.*, 2006) and fluid transport processes (Joseph and Miller, 1992; Peterson et al., 1997; Quinn et al., 2001). Lipofuscin accumulation is a by-product of phagocytosis (Feeney-Burns and Eldred, 1983; Rakoczy et al., 1996), and pH and Ca^{2+} are important mediators of purinergic and adrenergic signaling pathways that appear to play a role in RPE fluid transport (Joseph and Miller, 1992; Peterson et al., 1997; Quinn et al., 2001) (Fig. 15B). Defects in RPE phagocytosis are known to cause retinal degeneration (e.g., (LaVail, 1983)), and impaired fluid transport can cause serous retinal detachments (Marmor, 1990; Marmor and Yao, 1994; Negi and Marmor, 1983).

The process by which RPE phagocytose photoreceptor outer segments (POS) is complex, and can be divided into several stages (Bok, 1985; Feeney-Burns and Eldred, 1983; Finnemann *et al.*, 1997; Marmorstein *et al.*, 1998). The first is binding of POS to the RPE apical membrane. This is followed by internalization of the bound POS (Fig. 15B, 1). Upon internalization the nascent phagosome undergoes acidification and lysosomal enzymes are delivered from the ER (Fig. 15B, 2) resulting in a mature phagolysosome. Under normal circumstances the POS are, for the most part, degraded (Fig. 15B, 3). Lipofuscin is non-degradable material that remains in the latent phagosome and accumulates slowly in the RPE cell with age (Sparrow and Boulton, 2005). An important component of lipofuscin is A2E (Eldred, 1993; Eldred and Lasky, 1993), the levels of which are elevated in BVMD donor eyes (Bakall et al., 2007). The formation of A2E and other lipofuscin components is dependent on the presence of vitamin A, light, lysosomal enzymes, and pH (Ben-Shabat *et al.*, 2002; Bui *et al.*, 2006; Kim *et al.*, 2007; Liu *et al.*, 2000; Radu *et al.*, 2008; Sparrow *et al.*, 2008; Weng *et al.*, 1999). Thus, changes in the rate of acidification of the phagosome or the delivery of lysosomal enzymes could increase the rate of formation of A2E from precursors present in the engulfed POS. Best1 dysfunction causes changes in both pHi and Ca^{2+} homeostasis, and can alter Ca2+ signaling resulting from ligand activation of a GPCR (Fig. 15A, 2,3). Ca^{2+} is an important regulator in the early phases of phagocytosis by neutrophils and monocytes, and the phagocytic pathway used by the RPE is remarkably similar to that used for phagocytosis of apoptotic cells by neutrophils and monocytes (Finnemann and Rodriguez-Boulan, 1999). Best1 alters intracellular Ca^{2+} and interacts physically and functionally with VDCCs. VDCCs can regulate the uptake of OS by RPE cells (Karl et al., 2008), and changes in $[Ca^{2+}]_I$ are likely involved in OS binding and uptake, as well as on the delivery of lysosomal enzymes or fusion of nascent phagosomes with pre-existing lysosomes (Fig. 15B, 1, 2). NHE also plays a role in phagocytic uptake in neutrophils and monocytes and we have found that Best1 mutants cause HCO_3^- dependent changes in NHE activity and alter the resting pHi of RPE cells (Fig. 15A, 4). It is possible that Best1 may affect OS uptake (Fig. 15B, 1) through its effects on NHE, Ca^{2+}, or both. As such, we propose that Best1 is a critical regulator of ion transport and homeostasis via its effects on [Ca^{2+}]i and pHi and that lipofuscin accumulation (Fig. 14B, 5) and fluid transport defects result from Best1 dysfunction, not loss of Best1 function.

8. Future Directions

The function of the bestrophins remains controversial and incompletely understood. We have reviewed animal model data and findings from human diseases. There is no doubt that the potential Cl^- channel functions of the bestrophins are supported by a great deal of *in vitro* data [most recently reviewed in (Hartzell et al., 2008a)]. From that perspective, it is imperative that we understand the relationship between the bestrophins and the whole cell Cl^- currents associated with them. Are these currents passing directly through bestrophin channels? Does Best1 really "prefer" HCO_3^-? A lack of specific inhibitors of Best1 currents has been a major impediment to obtaining unquestioned single channel recordings from any putative bestrophin channel. Yet, changes in the ion selectivity of these conductances resulting from specific site-directed mutations in bestrophins suggest that they are components of some kind of ion (Cl^-, HCO_3^-, general anion) channel (Hartzell et al., 2008a). Resolving this dilemma would greatly aid our understanding of the role of bestrophins in tissues, could explain the HCO_3^- dependence that we have observed on NHE activity, and contribute to the development of specific screens for compounds that affect bestrophin function and may therefore be of therapeutic value in human disease.

It is also apparent that Best1 can affect Ca^{2+} transport, homeostasis, and signaling, as well as pHi. These properties are critical to the health of all cell types, and would seem more likely to underlie the clinical and histopathologic presentations of BVMD and the other bestrophinopathies, by accounting for the major histopathologic findings in these diseases; lipofuscin accumulation and potentially defective fluid transport. BVMD and AVMD in particular, have long been recognized as disorders that arise from RPE dysfunction. Linking the Ca^{2+} and pH regulatory functions of Best1 to bestrophin channel activity might provide a means to screen for compounds that interact specifically with bestrophins. If the functions are not linked, then understanding the basis of this dilemma becomes paramount. This effort will require extensive activity at the level of patch clamp electrophysiology. Animal models of bestrophinopathies will continue to be important tools for testing the hypothesis that the presentation of these diseases results from bestrophin dysfunction that causes changes in Ca^{2+} and pH homeostasis. We remain optimistic that these efforts will converge upon the development of an effective therapy for bestrophinopathies and diseases that involve the proteins that bestrophins interact with.

Acknowledgments

The authors thank Drs. L. Marmorstein, Y. Zhang, B. McKay, and W. D. Stamer for critically reading the manuscript. Work in the author's labs is funded by grants from the NIH (EY13160 to ADM), the Macular Vision Research Foundation (ADM), ALCON (ADM), VA Medical Research Service (NSP), Foundation Fighting Blindness (NSP) and unrestricted grants from Research to Prevent Blindness to the Department of Ophthalmology and Vision Science at the University of Arizona and to the Department of Ophthalmology, Cleveland Clinic Lerner College of Medicine of Case Western Reserve University.

References

Abernethy DR, Schwartz JB. Calcium-antagonist drugs. N Engl J Med 1999;341:1447–1457. [PubMed: 10547409]

Agbaga MP, Brush RS, Mandal MN, Henry K, Elliott MH, Anderson RE. Role of Stargardt-3 macular dystrophy protein (ELOVL4) in the biosynthesis of very long chain fatty acids. Proc Natl Acad Sci U S A 2008;105:12843–12848. [PubMed: 18728184]

Al-Jumaily M, Kozlenkov A, Mechaly I, Fichard A, Matha V, Scamps F, Valmier J, Carroll P. Expression of three distinct families of calcium-activated chloride channel genes in the mouse dorsal root ganglion. Neurosci Bull 2007;23:293–299. [PubMed: 17952139]

Allen DG, Cairns SP, Turvey SE, Lee JA. Intracellular calcium and myocardial function during ischemia. Adv Exp Med Biol 1993;346:19–29. [PubMed: 8184757]

Allen DG, Lee JA, Smith GL. The consequences of simulated ischaemia on intracellular Ca2+ and tension in isolated ferret ventricular muscle. J Physiol 1989;410:297–323. [PubMed: 2795481]

Allen DG, Xiao XH. Role of the cardiac Na+/H+ exchanger during ischemia and reperfusion. Cardiovasc Res 2003;57:934–941. [PubMed: 12650871]

Allikmets R, Seddon JM, Bernstein PS, Hutchinson A, Atkinson A, Sharma S, Gerrard B, Li W, Metzker ML, Wadelius C, Caskey CT, Dean M, Petrukhin K. Evaluation of the Best disease gene in patients with age-related macular degeneration and other maculopathies. Hum Genet 1999;104:449–453. [PubMed: 10453731]

Arden GB, Barrada A, Kelsey JH. New Clinical Test of Retinal Function Based Upon the Standing Potential of the Eye. Br J Ophthalmol 1962;46:449–467. [PubMed: 18170802]

Arden GB, Kelsey JH. Changes produced by light in the standing potential of the human eye. J Physiol 1962a;161:189–204. [PubMed: 13862112]

Arden GB, Kelsey JH. Some observations on the relationship between the standing potential of the human eye and the bleaching and regeneration of visual purple. J Physiol 1962b;161:205–226. [PubMed: 14036845]

Bakall B, Marknell T, Ingvast S, Koisti MJ, Sandgren O, Li W, Bergen AA, Andreasson S, Rosenberg T, Petrukhin K, Wadelius C. The mutation spectrum of the bestrophin protein--functional implications. Hum Genet 1999;104:383–389. [PubMed: 10394929]

Bakall B, Marmorstein LY, Hoppe G, Peachey NS, Wadelius C, Marmorstein AD. Expression and localization of bestrophin during normal mouse development. Invest Ophthalmol Vis Sci 2003;44:3622–3628. [PubMed: 12882816]

Bakall B, McLaughlin P, Stanton JB, Zhang Y, Hartzell HC, Marmorstein LY, Marmorstein AD. Bestrophin-2 is involved in the generation of intraocular pressure. Invest Ophthalmol Vis Sci 2008;49:1563–1570. [PubMed: 18385076]

Bakall B, Radu RA, Stanton JB, Burke JM, McKay BS, Wadelius C, Mullins RF, Stone EM, Travis GH, Marmorstein AD. Enhanced accumulation of A2E in individuals homozygous or heterozygous for mutations in BEST1 (VMD2). Exp Eye Res 2007;85:34–43. [PubMed: 17477921]

Ball SL, Pardue MT, McCall MA, Gregg RG, Peachey NS. Immunohistochemical analysis of the outer plexiform layer in the nob mouse shows no abnormalities. Vis Neurosci 2003;20:267–272. [PubMed: 14570248]

Bard LA, Cross HE. Genetic counseling of families with Best macular dystrophy. Trans Sect Ophthalmol Am Acad Ophthalmol Otolaryngol 1975;79:OP865–873.

Barro Soria R, Spitzner M, Schreiber R, Kunzelmann K. Bestrophin 1 enables Ca2+ activated Cl- conductance in epithelia. J Biol Chem. 2006

Barro-Soria R, Schreiber R, Kunzelmann K. Bestrophin 1 and 2 are components of the Ca(2+) activated Cl(-) conductance in mouse airways. Biochim Biophys Acta 2008;1783:1993–2000. [PubMed: 18652850]

Ben-Shabat S, Parish CA, Vollmer HR, Itagaki Y, Fishkin N, Nakanishi K, Sparrow JR. Biosynthetic studies of A2E, a major fluorophore of retinal pigment epithelial lipofuscin. J Biol Chem 2002;277:7183–7190. [PubMed: 11756445]

Best F. Uber eine hereditare Maculaaffektion Beitrag zur Vererbungslehre. Z Augenheilk 1905;13:199–212.

Birol G, Wang S, Budzynski E, Wangsa-Wirawan ND, Linsenmeier RA. Oxygen distribution and consumption in the macaque retina. Am J Physiol Heart Circ Physiol 2007;293:H1696–1704. [PubMed: 17557923]

Bishara SA, Matamoros N. Evaluation of several tests in screening for chloroquine maculopathy. Eye 1989;3(Pt 6):777–782. [PubMed: 2630362]

Blodi CF, Stone EM. Best's vitelliform dystrophy. Ophthalmic Paediatr Genet 1990;11:49–59. [PubMed: 2190134]

Bok D. Retinal photoreceptor-pigment epithelium interactions. Friedenwald lecture. Invest Ophthalmol Vis Sci 1985;26:1659–1694. [PubMed: 2933359]

Boon CJ, Klevering BJ, den Hollander AI, Zonneveld MN, Theelen T, Cremers FP, Hoyng CB. Clinical and genetic heterogeneity in multifocal vitelliform dystrophy. Arch Ophthalmol 2007;125:1100–1106. [PubMed: 17698758]

Brake AJ, Julius D. Signaling by extracellular nucleotides. Annu Rev Cell Dev Biol 1996;12:519–541. [PubMed: 8970736]

Brown M, Marmor M, Vaegan, Zrenner E, Brigell M, Bach M. ISCEV Standard for Clinical Electro-oculography (EOG) 2006. Doc Ophthalmol 2006;113:205–212. [PubMed: 17109157]

Bui TV, Han Y, Radu RA, Travis GH, Mata NL. Characterization of native retinal fluorophores involved in biosynthesis of A2E and lipofuscin-associated retinopathies. J Biol Chem 2006;281:18112–18119. [PubMed: 16638746]

Burgess DL, Jones JM, Meisler MH, Noebels JL. Mutation of the Ca2+ channel beta subunit gene Cchb4 is associated with ataxia and seizures in the lethargic (lh) mouse. Cell 1997;88:385–392. [PubMed: 9039265]

Burgess R, Maclaren R, Davidson A, Urquhart J, Holder G, Robson A, Moore A, R OK, Black G, Manson F. ADVIRC is caused by distinct mutations in BEST1 that alter pre-mRNA splicing. J Med Genet. 2008a

Burgess R, Millar ID, Leroy BP, Urquhart JE, Fearon IM, De Baere E, Brown PD, Robson AG, Wright GA, Kestelyn P, Holder GE, Webster AR, Manson FD, Black GC. Biallelic mutation of BEST1 causes a distinct retinopathy in humans. Am J Hum Genet 2008b;82:19–31. [PubMed: 18179881]

Caldwell GM, Kakuk LE, Griesinger IB, Simpson SA, Nowak NJ, Small KW, Maumenee IH, Rosenfeld PJ, Sieving PA, Shows TB, Ayyagari R. Bestrophin gene mutations in patients with Best vitelliform macular dystrophy. Genomics 1999;58:98–101. [PubMed: 10331951]

Caputo A, Caci E, Ferrera L, Pedemonte N, Barsanti C, Sondo E, Pfeffer U, Ravazzolo R, Zegarra-Moran O, Galietta LJ. TMEM16A, a membrane protein associated with calcium-dependent chloride channel activity. Science 2008;322:590–594. [PubMed: 18772398]

Carter-Dawson LD, LaVail MM. Rods and cones in the mouse retina. I. Structural analysis using light and electron microscopy. J Comp Neurol 1979;188:245–262. [PubMed: 500858]

Chang B, Hawes NL, Hurd RE, Davisson MT, Nusinowitz S, Heckenlively JR. Retinal degeneration mutants in the mouse. Vision Res 2002;42:517–525. [PubMed: 11853768]

Chien LT, Zhang ZR, Hartzell HC. Single Cl- channels activated by Ca2+ in Drosophila S2 cells are mediated by bestrophins. J Gen Physiol 2006;128:247–259. [PubMed: 16940553]

Chung JE, Spaide RF. Fundus autofluorescence and vitelliform macular dystrophy. Arch Ophthalmol 2004;122:1078–1079. [PubMed: 15249383]

Cross HE, Bard L. Electro-oculography in Best's macular dystrophy. Am J Ophthalmol 1974;77:46–50. [PubMed: 4824173]

Dalke C, Graw J. Mouse mutants as models for congenital retinal disorders. Exp Eye Res 2005;81:503–512. [PubMed: 16026784]

Dawis SM, Niemeyer G. Dopamine influences the light peak in the perfused mammalian eye. Invest Ophthalmol Vis Sci 1986;27:330–335. [PubMed: 3005190]

Deguchi J, Yamamoto A, Yoshimori T, Sugasawa K, Moriyama Y, Futai M, Suzuki T, Kato K, Uyama M, Tashiro Y. Acidification of phagosomes and degradation of rod outer segments in rat retinal pigment epithelium. Invest Ophthalmol Vis Sci 1994;35:568–579. [PubMed: 8113008]

Duta V, Duta F, Puttagunta L, Befus AD, Duszyk M. Regulation of basolateral Cl(-) channels in airway epithelial cells: the role of nitric oxide. J Membr Biol 2006;213:165–174. [PubMed: 17468957]

Duta V, Szkotak AJ, Nahirney D, Duszyk M. The role of bestrophin in airway epithelial ion transport. FEBS Lett 2004;577:551–554. [PubMed: 15556645]

Eldred GE. Age pigment structure. Nature 1993;364:396. [PubMed: 8332209]

Eldred GE, Lasky MR. Retinal age pigments generated by self-assembling lysosomotropic detergents. Nature 1993;361:724–726. [PubMed: 8441466]

Elliott AC, Smith GL, Eisner DA, Allen DG. Metabolic changes during ischaemia and their role in contractile failure in isolated ferret hearts. J Physiol 1992;454:467–490. [PubMed: 1474498]

Esumi N, Oshima Y, Li Y, Campochiaro PA, Zack DJ. Analysis of the VMD2 promoter and implication of E-box binding factors in its regulation. J Biol Chem 2004;279:19064–19073. [PubMed: 14982938]

Feeney-Burns L, Eldred GE. The fate of the phagosome: conversion to ‘age pigment’ and impact in human retinal pigment epithelium. Trans Ophthalmol Soc U K 1983;103(Pt 4):416–421. [PubMed: 6589859]

Felbor U, Schilling H, Weber BH. Adult vitelliform macular dystrophy is frequently associated with mutations in the peripherin/RDS gene. Hum Mutat 1997;10:301–309. [PubMed: 9338584]

Finnemann SC, Bonilha VL, Marmorstein AD, Rodriguez-Boulan E. Phagocytosis of rod outer segments by retinal pigment epithelial cells requires alpha(v)beta5 integrin for binding but not for internalization. Proc Natl Acad Sci U S A 1997;94:12932–12937. [PubMed: 9371778]

Finnemann SC, Rodriguez-Boulan E. Macrophage and retinal pigment epithelium phagocytosis: apoptotic cells and photoreceptors compete for alphavbeta3 and alphavbeta5 integrins, and protein kinase C regulates alphavbeta5 binding and cytoskeletal linkage. J Exp Med 1999;190:861–874. [PubMed: 10499924]

Fishman GA, Baca W, Alexander KR, Derlacki DJ, Glenn AM, Viana M. Visual acuity in patients with best vitelliform macular dystrophy. Ophthalmology 1993;100:1665–1670. [PubMed: 8233392]

Foulds WS, Ikeda H. The effects of detachment of the retina on induced and resting ocular potentials in the rabbit. Invest Ophthalmol Vis Sci 1966;5:93–108.

Frangieh GT, Green WR, Fine SL. A histopathologic study of Best's macular dystrophy. Arch Ophthalmol 1982;100:1115–1121. [PubMed: 7092655]

Fries JE, Wheeler-Schilling TH, Guenther E, Kohler K. Expression of P2Y1, P2Y2, P2Y4, and P2Y6 receptor subtypes in the rat retina. Invest Ophthalmol Vis Sci 2004;45:3410–3417. [PubMed: 15452043]

Fujii S, Gallemore RP, Hughes BA, Steinberg RH. Direct evidence for a basolateral membrane Cl-conductance in toad retinal pigment epithelium. Am J Physiol 1992;262:C374–383. [PubMed: 1311500]

Gallemore, RP.; Hughes, BA.; Miller, SS. Light Induced responses of the Retinal Pigment Epithelium. In: Marmor, MF.; Wolfensberger, TJ., editors. The Retinal Pigment Epithelium. Oxford University Press; New York: 1998. p. 175-198.

Gallemore RP, Steinberg RH. Effects of DIDS on the chick retinal pigment epithelium. II. Mechanism of the light peak and other responses originating at the basal membrane. J Neurosci 1989;9:1977–1984. [PubMed: 2723762]

Gallemore RP, Steinberg RH. Effects of dopamine on the chick retinal pigment epithelium. Membrane potentials and light-evoked responses. Invest Ophthalmol Vis Sci 1990;31:67–80. [PubMed: 2298543]

Gallemore RP, Steinberg RH. Light-evoked modulation of basolateral membrane Cl- conductance in chick retinal pigment epithelium: the light peak and fast oscillation. J Neurophysiol 1993;70:1669–1680. [PubMed: 8283222]

Goldberg MF, Lee FL, Tso MO, Fishman GA. Histopathologic study of autosomal dominant vitreoretinochoroidopathy. Peripheral annular pigmentary dystrophy of the retina. Ophthalmology 1989;96:1736–1746. [PubMed: 2516300]

Gomez A, Cedano J, Oliva B, Pinol J, Querol E. The gene causing the Best's macular dystrophy (BMD) encodes a putative ion exchanger. DNA Seq 2001;12:431–435. [PubMed: 11913792]

Gouras P, Gunkel RD. The Eog in Chloroquine and Other Retinopathies. Arch Ophthalmol 1963;70:629–639. [PubMed: 14057692]

Guziewicz KE, Zangerl B, Lindauer SJ, Mullins RF, Sandmeyer LS, Grahn BH, Stone EM, Acland GM, Aguirre GD. Bestrophin gene mutations cause canine multifocal retinopathy: a novel animal model for best disease. Invest Ophthalmol Vis Sci 2007;48:1959–1967. [PubMed: 17460247]

Hagen AR, Barabote RD, Saier MH. The bestrophin family of anion channels: identification of prokaryotic homologues. Mol Membr Biol 2005;22:291–302. [PubMed: 16154901]

Hall MO, Abrams TA, Mittag TW. ROS ingestion by RPE cells is turned off by increased protein kinase C activity and by increased calcium. Exp Eye Res 1991;52:591–598. [PubMed: 2065727]

Han DP, Burke JM, Blair JR, Simons KB. Histopathologic study of autosomal dominant vitreoretinochoroidopathy in a 26-year-old woman. Arch Ophthalmol 1995;113:1561–1566. [PubMed: 7487628]

Hartzell C, Qu Z, Putzier I, Artinian L, Chien LT, Cui Y. Looking chloride channels straight in the eye: bestrophins, lipofuscinosis, and retinal degeneration. Physiology (Bethesda) 2005;20:292–302. [PubMed: 16174869]

Hartzell HC, Qu Z, Yu K, Xiao Q, Chien LT. Molecular physiology of bestrophins: multifunctional membrane proteins linked to best disease and other retinopathies. Physiol Rev 2008a;88:639–672. [PubMed: 18391176]

Hartzell HC, Yu K, Xiao Q, Chien LT, Qu Z. Anoctamin / TMEM16 family members are Ca2+-activated Cl- channels. J Physiol. 2008b

Haugh LM, Linsenmeier RA, Goldstick TK. Mathematical models of the spatial distribution of retinal oxygen tension and consumption, including changes upon illumination. Ann Biomed Eng 1990;18:19–36. [PubMed: 2306030]

Hu J, Bok D. A cell culture medium that supports the differentiation of human retinal pigment epithelium into functionally polarized monolayers. Mol Vis 2001;7:14–19. [PubMed: 11182021]

Jarc-Vidmar M, Kraut A, Hawlina M. Fundus autofluorescence imaging in Best's vitelliform dystrophy. Klin Monatsbl Augenheilkd 2003;220:861–867. [PubMed: 14704944]

Joseph DP, Miller SS. Alpha-1-adrenergic modulation of K and Cl transport in bovine retinal pigment epithelium. J Gen Physiol 1992;99:263–290. [PubMed: 1319462]

Kaemmerer E, Schutt F, Krohne TU, Holz FG, Kopitz J. Effects of lipid peroxidation-related protein modifications on RPE lysosomal functions and POS phagocytosis. Invest Ophthalmol Vis Sci 2007;48:1342–1347. [PubMed: 17325182]

Karan G, Lillo C, Yang Z, Cameron DJ, Locke KG, Zhao Y, Thirumalaichary S, Li C, Birch DG, Vollmer-Snarr HR, Williams DS, Zhang K. Lipofuscin accumulation, abnormal electrophysiology, and photoreceptor degeneration in mutant ELOVL4 transgenic mice: a model for macular degeneration. Proc Natl Acad Sci U S A 2005;102:4164–4169. [PubMed: 15749821]

Karl MO, Kroeger W, Wimmers S, Milenkovic VM, Valtink M, Engelmann K, Strauss O. Endogenous Gas6 and Ca2+ -channel activation modulate phagocytosis by retinal pigment epithelium. Cell Signal 2008;20:1159–1168. [PubMed: 18395422]

Karmazyn M, Sostaric JV, Gan XT. The myocardial Na+/H+ exchanger: a potential therapeutic target for the prevention of myocardial ischaemic and reperfusion injury and attenuation of postinfarction heart failure. Drugs 2001;61:375–389. [PubMed: 11293648]

Kaufman SJ, Goldberg MF, Orth DH, Fishman GA, Tessler H, Mizuno K. Autosomal dominant vitreoretinochoroidopathy. Arch Ophthalmol 1982;100:272–278. [PubMed: 7065944]

Keeler CE. The Inheritance of a Retinal Abnormality in White Mice. Proc Natl Acad Sci U S A 1924;10:329–333. [PubMed: 16576828]

Khosravani H, Zamponi GW. Voltage-gated calcium channels and idiopathic generalized epilepsies. Physiol Rev 2006;86:941–966. [PubMed: 16816142]

Kikawada N. Variations in the corneo-retinal standing potential of the vertebrate eye during light and dark adaptations. Jpn J Physiol 1968;18:687–702. [PubMed: 5305288]

Kim SR, Jang YP, Jockusch S, Fishkin NE, Turro NJ, Sparrow JR. The all-trans-retinal dimer series of lipofuscin pigments in retinal pigment epithelial cells in a recessive Stargardt disease model. Proc Natl Acad Sci U S A 2007;104:19273–19278. [PubMed: 18048333]

Kim SR, Nakanishi K, Itagaki Y, Sparrow JR. Photooxidation of A2-PE, a photoreceptor outer segment fluorophore, and protection by lutein and zeaxanthin. Exp Eye Res 2006;82:828–839. [PubMed: 16364293]

Kramer F, Mohr N, Kellner U, Rudolph G, Weber BH. Ten novel mutations in VMD2 associated with Best macular dystrophy (BMD). Hum Mutat 2003;22:418. [PubMed: 14517959]

Kramer F, Stohr H, Weber BH. Cloning and characterization of the murine Vmd2 RFP-TM gene family. Cytogenet Genome Res 2004;105:107–114. [PubMed: 15218265]

Kramer F, White K, Pauleikhoff D, Gehrig A, Passmore L, Rivera A, Rudolph G, Kellner U, Andrassi M, Lorenz B, Rohrschneider K, Blankenagel A, Jurklies B, Schilling H, Schutt F, Holz FG, Weber BH. Mutations in the VMD2 gene are associated with juvenile-onset vitelliform macular dystrophy (Best disease) and adult vitelliform macular dystrophy but not age-related macular degeneration. Eur J Hum Genet 2000;8:286–292. [PubMed: 10854112]

Lafaut BA, Loeys B, Leroy BP, Spileers W, De Laey JJ, Kestelyn P. Clinical and electrophysiological findings in autosomal dominant vitreoretinochoroidopathy: report of a new pedigree. Graefes Arch Clin Exp Ophthalmol 2001;239:575–582. [PubMed: 11585313]

Lang K, Wagner C, Haddad G, Burnekova O, Geibel J. Intracellular pH activates membrane-bound Na (+)/H(+) exchanger and vacuolar H(+)-ATPase in human embryonic kidney (HEK) cells. Cell Physiol Biochem 2003;13:257–262. [PubMed: 14586169]

LaVail MM. Outer segment disc shedding and phagocytosis in the outer retina. Trans Ophthalmol Soc U K 1983;103(Pt 4):397–404. [PubMed: 6380008]

Lee JA, Allen DG. Changes in intracellular free calcium concentration during long exposures to simulated ischemia in isolated mammalian ventricular muscle. Circ Res 1992;71:58–69. [PubMed: 1606668]

Liu J, Itagaki Y, Ben-Shabat S, Nakanishi K, Sparrow JR. The biosynthesis of A2E, a fluorophore of aging retina, involves the formation of the precursor, A2-PE, in the photoreceptor outer segment membrane. J Biol Chem 2000;275:29354–29360. [PubMed: 10887199]

Liu J, Lu W, Reigada D, Nguyen J, Laties AM, Mitchell CH. Restoration of lysosomal pH in RPE cells from cultured human and ABCA4(-/-) mice: pharmacologic approaches and functional recovery. Invest Ophthalmol Vis Sci 2008;49:772–780. [PubMed: 18235027]

Luo J, Chen H, Kintner DB, Shull GE, Sun D. Decreased neuronal death in Na+/H+ exchanger isoform 1-null mice after in vitro and in vivo ischemia. J Neurosci 2005;25:11256–11268. [PubMed: 16339021]

Maminishkis A, Chen S, Jalickee S, Banzon T, Shi G, Wang FE, Ehalt T, Hammer JA, Miller SS. Confluent monolayers of cultured human fetal retinal pigment epithelium exhibit morphology and physiology of native tissue. Invest Ophthalmol Vis Sci 2006;47:3612–3624. [PubMed: 16877436]

Marmor MF. “Vitelliform” lesions in adults. Ann Ophthalmol 1979;11:1705–1712. [PubMed: 556129]

Marmor MF. Control of subretinal fluid: experimental and clinical studies. Eye 1990;4(Pt 2):340–344. [PubMed: 2199242]

Marmor MF, Yao XY. Conditions necessary for the formation of serous detachment. Experimental evidence from the cat. Arch Ophthalmol 1994;112:830–838. [PubMed: 8002843]

Marmorstein AD, Finnemann SC, Bonilha VL, Rodriguez-Boulan E. Morphogenesis of the retinal pigment epithelium: toward understanding retinal degenerative diseases. Ann N Y Acad Sci 1998;857:1–12. [PubMed: 9917828]

Marmorstein AD, Kinnick TR. Focus on molecules: bestrophin (best-1). Exp Eye Res 2007;85:423–424. [PubMed: 16720022]

Marmorstein AD, Marmorstein LY. The challenge of modeling macular degeneration in mice. Trends Genet 2007;23:225–231. [PubMed: 17368622]

Marmorstein AD, Marmorstein LY, Rayborn M, Wang X, Hollyfield JG, Petrukhin K. Bestrophin, the product of the Best vitelliform macular dystrophy gene (VMD2), localizes to the basolateral plasma membrane of the retinal pigment epithelium. Proc Natl Acad Sci U S A 2000;97:12758–12763. [PubMed: 11050159]

Marmorstein AD, Peachey NS, Csaky KG. In vivo gene transfer as a means to study the physiology and morphogenesis of the retinal pigment epithelium in the rat. Methods 2003;30:277–285. [PubMed: 12798142]

Marmorstein AD, Stanton JB, Yocom J, Bakall B, Schiavone MT, Wadelius C, Marmorstein LY, Peachey NS. A model of best vitelliform macular dystrophy in rats. Invest Ophthalmol Vis Sci 2004;45:3733–3739. [PubMed: 15452084]

Marmorstein LY, McLaughlin PJ, Stanton JB, Yan L, Crabb JW, Marmorstein AD. Bestrophin interacts physically and functionally with protein phosphatase 2A. J Biol Chem 2002;277:30591–30597. [PubMed: 12058047]

Marmorstein LY, Wu J, McLaughlin P, Yocom J, Karl MO, Neussert R, Wimmers S, Stanton JB, Gregg RG, Strauss O, Peachey NS, Marmorstein AD. The light peak of the electroretinogram is dependent on voltage-gated calcium channels and antagonized by bestrophin (best-1). J Gen Physiol 2006;127:577–589. [PubMed: 16636205]

Marquardt A, Stohr H, Passmore LA, Kramer F, Rivera A, Weber BH. Mutations in a novel gene, VMD2, encoding a protein of unknown properties cause juvenile-onset vitelliform macular dystrophy (Best's disease). Hum Mol Genet 1998;7:1517–1525. [PubMed: 9700209]

Masuoka H, Fujimori K, Sekiguchi S, Watanabe M, Wang H, Aiso T, Yamaya H, Satoh A, Satomi S. Beneficial effect of FR183998, a Na+/H+ exchanger inhibitor, on porcine pancreas

allotransplantation retrieved from non-heart-beating donors. Transplant Proc 2005;37:223–225. [PubMed: 15808601]

Mentzer RM Jr, Bartels C, Bolli R, Boyce S, Buckberg GD, Chaitman B, Haverich A, Knight J, Menasche P, Myers ML, Nicolau J, Simoons M, Thulin L, Weisel RD. Sodium-hydrogen exchange inhibition by cariporide to reduce the risk of ischemic cardiac events in patients undergoing coronary artery bypass grafting: results of the EXPEDITION study. Ann Thorac Surg 2008;85:1261–1270. [PubMed: 18355507]

Milenkovic VM, Langmann T, Schreiber R, Kunzelmann K, Weber BH. Molecular evolution and functional divergence of the bestrophin protein family. BMC Evol Biol 2008;8:72. [PubMed: 18307799]

Milenkovic VM, Rivera A, Horling F, Weber BH. Insertion and topology of normal and mutant bestrophin-1 in the endoplasmic reticulum membrane. J Biol Chem 2007;282:1313–1321. [PubMed: 17110374]

Mohler CW, Fine SL. Long-term evaluation of patients with Best's vitelliform dystrophy. Ophthalmology 1981;88:688–692. [PubMed: 7267039]

Mullins RF, Kuehn MH, Faidley EA, Syed NA, Stone EM. Differential macular and peripheral expression of bestrophin in human eyes and its implication for best disease. Invest Ophthalmol Vis Sci 2007;48:3372–3380. [PubMed: 17591911]

Mullins RF, Oh KT, Heffron E, Hageman GS, Stone EM. Late development of vitelliform lesions and flecks in a patient with best disease: clinicopathologic correlation. Arch Ophthalmol 2005;123:1588–1594. [PubMed: 16286623]

Nao-i N, Nilsson SE, Gallemore RP, Steinberg RH. Effects of melatonin on the chick retinal pigment epithelium: membrane potentials and light-evoked responses. Exp Eye Res 1989;49:573–589. [PubMed: 2806426]

Negi A, Marmor MF. The resorption of subretinal fluid after diffuse damage to the retinal pigment epithelium. Invest Ophthalmol Vis Sci 1983;24:1475–1479. [PubMed: 6642927]

Nordstrom S, Thorburn W. Dominantly inherited macular degeneration (Best's disease) in a homozygous father with 11 children. Clin Genet 1980;18:211–216. [PubMed: 7438501]

O'Driscoll KE, Hatton WJ, Burkin HR, Leblanc N, Britton FC. Expression, localization, and functional properties of Bestrophin 3 channel isolated from mouse heart. Am J Physiol Cell Physiol 2008;295:C1610–1624. [PubMed: 18945938]

O'Gorman S, Flaherty WA, Fishman GA, Berson EL. Histopathologic findings in Best's vitelliform macular dystrophy. Arch Ophthalmol 1988;106:1261–1268. [PubMed: 3415551]

Pacione LR, Szego MJ, Ikeda S, Nishina PM, McInnes RR. Progress toward understanding the genetic and biochemical mechanisms of inherited photoreceptor degenerations. Annu Rev Neurosci 2003;26:657–700. [PubMed: 14527271]

Park CO, Xiao XH, Allen DG. Changes in intracellular Na+ and pH in rat heart during ischemia: role of Na+/H+ exchanger. Am J Physiol 1999;276:H1581–1590. [PubMed: 10330242]

Peachey NS, Stanton JB, Marmorstein AD. Noninvasive recording and response characteristics of the rat dc-electroretinogram. Vis Neurosci 2002;19:693–701. [PubMed: 12688665]

Peters S, Reinthal E, Blitgen-Heinecke P, Bartz-Schmidt KU, Schraermeyer U. Inhibition of lysosomal degradation in retinal pigment epithelium cells induces exocytosis of phagocytic residual material at the basolateral plasma membrane. Ophthalmic Res 2006;38:83–88. [PubMed: 16352920]

Peterson WM, Meggyesy C, Yu K, Miller SS. Extracellular ATP activates calcium signaling, ion, and fluid transport in retinal pigment epithelium. J Neurosci 1997;17:2324–2337. [PubMed: 9065493]

Petrukhin K, Koisti MJ, Bakall B, Li W, Xie G, Marknell T, Sandgren O, Forsman K, Holmgren G, Andreasson S, Vujic M, Bergen AA, McGarty-Dugan V, Figueroa D, Austin CP, Metzker ML, Caskey CT, Wadelius C. Identification of the gene responsible for Best macular dystrophy. Nat Genet 1998;19:241–247. [PubMed: 9662395]

Pianta MJ, Aleman TS, Cideciyan AV, Sunness JS, Li Y, Campochiaro BA, Campochiaro PA, Zack DJ, Stone EM, Jacobson SG. In vivo micropathology of Best macular dystrophy with optical coherence tomography. Exp Eye Res 2003;76:203–211. [PubMed: 12565808]

Pifferi S, Pascarella G, Boccaccio A, Mazzatenta A, Gustincich S, Menini A, Zucchelli S. Bestrophin-2 is a candidate calcium-activated chloride channel involved in olfactory transduction. Proc Natl Acad Sci U S A 2006;103:12929–12934. [PubMed: 16912113]

Piper HM, Balser C, Ladilov YV, Schafer M, Siegmund B, Ruiz-Meana M, Garcia-Dorado D. The role of Na+/H+ exchange in ischemia-reperfusion. Basic Res Cardiol 1996;91:191–202. [PubMed: 8831938]

Piper HM, Meuter K, Schafer C. Cellular mechanisms of ischemia-reperfusion injury. Ann Thorac Surg 2003;75:S644–648. [PubMed: 12607706]

Qu Z, Chien LT, Cui Y, Hartzell HC. The anion-selective pore of the bestrophins, a family of chloride channels associated with retinal degeneration. J Neurosci 2006;26:5411–5419. [PubMed: 16707793]

Qu Z, Fischmeister R, Hartzell C. Mouse bestrophin-2 is a bona fide Cl(-) channel: identification of a residue important in anion binding and conduction. J Gen Physiol 2004;123:327–340. [PubMed: 15051805]

Qu Z, Hartzell C. Determinants of anion permeation in the second transmembrane domain of the mouse bestrophin-2 chloride channel. J Gen Physiol 2004;124:371–382. [PubMed: 15452198]

Qu Z, Hartzell HC. Bestrophin Cl- channels are highly permeable to HCO3. Am J Physiol Cell Physiol 2008;294:C1371–1377. [PubMed: 18400985]

Qu Z, Wei RW, Mann W, Hartzell HC. Two bestrophins cloned from Xenopus laevis oocytes express Ca(2+)-activated Cl(-) currents. J Biol Chem 2003;278:49563–49572. [PubMed: 12939260]

Quinn RH, Quong JN, Miller SS. Adrenergic receptor activated ion transport in human fetal retinal pigment epithelium. Invest Ophthalmol Vis Sci 2001;42:255–264. [PubMed: 11133877]

Radu RA, Mata NL, Bagla A, Travis GH. Light exposure stimulates formation of A2E oxiranes in a mouse model of Stargardt's macular degeneration. Proc Natl Acad Sci U S A 2004;101:5928–5933. [PubMed: 15067110]

Radu RA, Yuan Q, Hu J, Peng JH, Lloyd M, Nusinowitz S, Bok D, Travis GH. Accelerated accumulation of lipofuscin pigments in the RPE of a mouse model for ABCA4-mediated retinal dystrophies following Vitamin A supplementation. Invest Ophthalmol Vis Sci 2008;49:3821–3829. [PubMed: 18515570]

Rakoczy PE, Baines M, Kennedy CJ, Constable IJ. Correlation between autofluorescent debris accumulation and the presence of partially processed forms of cathepsin D in cultured retinal pigment epithelial cells challenged with rod outer segments. Exp Eye Res 1996;63:159–167. [PubMed: 8983973]

Renner AB, Tillack H, Kraus H, Kramer F, Mohr N, Weber BH, Foerster MH, Kellner U. Late onset is common in best macular dystrophy associated with VMD2 gene mutations. Ophthalmology 2005;112:586–592. [PubMed: 15808248]

Rock JR, Futtner CR, Harfe BD. The transmembrane protein TMEM16A is required for normal development of the murine trachea. Dev Biol 2008;321:141–149. [PubMed: 18585372]

Roider J, Fritsch E, Hoerauf H, Heide W, Laqua H. Autosomal dominant vitreoretinochoroidopathy. Retina 1997;17:294–299. [PubMed: 9279944]

Rosenthal R, Bakall B, Kinnick T, Peachey N, Wimmers S, Wadelius C, Marmorstein A, Strauss O. Expression of bestrophin-1, the product of the VMD2 gene, modulates voltage-dependent Ca2+ channels in retinal pigment epithelial cells. FASEB J 2006;20:178–180. [PubMed: 16282372]

Schroeder BC, Cheng T, Jan YN, Jan LY. Expression cloning of TMEM16A as a calcium-activated chloride channel subunit. Cell 2008;134:1019–1029. [PubMed: 18805094]

Sodi A, Passerini I, Simonelli F, Testa F, Menchini U, Torricelli F. A novel mutation in the VMD2 gene in an Italian family with Best maculopathy. J Fr Ophtalmol 2007;30:616–620. [PubMed: 17646752]

Spaide RF, Noble K, Morgan A, Freund KB. Vitelliform macular dystrophy. Ophthalmology 2006;113:1392–1400. [PubMed: 16877078]

Sparrow JR, Boulton M. RPE lipofuscin and its role in retinal pathobiology. Exp Eye Res 2005;80:595–606. [PubMed: 15862166]

Sparrow JR, Kim SR, Cuervo AM, Bandhyopadhyayand U. A2E, a pigment of RPE lipofuscin, is generated from the precursor, A2PE by a lysosomal enzyme activity. Adv Exp Med Biol 2008;613:393–398. [PubMed: 18188969]

Srivastava A, Romanenko VG, Gonzalez-Begne M, Catalan MA, Melvin JE. A variant of the Ca2+-activated Cl channel Best3 is expressed in mouse exocrine glands. J Membr Biol 2008;222:43–54. [PubMed: 18414923]

Stanton JB, Goldberg AF, Hoppe G, Marmorstein LY, Marmorstein AD. Hydrodynamic properties of porcine bestrophin-1 in Triton X-100. Biochim Biophys Acta 2006;1758:241–247. [PubMed: 16600174]

Stanton JB, Wu J, McLaughlin PJ, Marmorstein LY, Peachey N, Marmorstein AD. A Comparison of the Phenotypes of Bestrophin Knock-In and Knock-Out Mice: Implications for the Pathogenesis of Best Vitelliform Macular Degeneration. Invest Ophthalmol Vis Sci 2008;49E-Abstract 5188

Steinberg RH. Interactions between the retinal pigment epithelium and the neural retina. Doc Ophthalmol 1985;60:327–346. [PubMed: 3905312]

Steinberg RH, Linsenmeier RA, Griff ER. Three light-evoked responses of the retinal pigment epithelium. Vision Res 1983;23:1315–1323. [PubMed: 6606894]

Stohr H, Marquardt A, Nanda I, Schmid M, Weber BH. Three novel human VMD2-like genes are members of the evolutionary highly conserved RFP-TM family. Eur J Hum Genet 2002;10:281–284. [PubMed: 12032738]

Strauss O, Milenkovic V, Striessnig J, Krejcova S. Direct Interaction of Bestrophin-1 and Beta-subunits of Voltage-Dependent Calcium Channels. Invest Ophthalmol Vis Sci 2008;49E-Abstract 5182

Sun H, Tsunenari T, Yau KW, Nathans J. The vitelliform macular dystrophy protein defines a new family of chloride channels. Proc Natl Acad Sci U S A 2002;99:4008–4013. [PubMed: 11904445]

Szel A, Rohlich P, Caffe AR, van Veen T. Distribution of cone photoreceptors in the mammalian retina. Microsc Res Tech 1996;35:445–462. [PubMed: 9016448]

ten Hove M, Jansen MA, Nederhoff MG, Van Echteld CJ. Combined blockade of the Na+ channel and the Na+/H+ exchanger virtually prevents ischemic Na+ overload in rat hearts. Mol Cell Biochem 2007;297:101–110. [PubMed: 17102905]

Thorburn W, Nordstrom S. EOG in a large family with hereditary macular degeneration. (Best's vitelliform macular dystrophy) identification of gene carriers. Acta Ophthalmol (Copenh) 1978;56:455–464. [PubMed: 581134]

Tsunenari T, Sun H, Williams J, Cahill H, Smallwood P, Yau KW, Nathans J. Structure-function analysis of the bestrophin family of anion channels. J Biol Chem 2003;278:41114–41125. [PubMed: 12907679]

Vasireddy V, Jablonski MM, Mandal MN, Raz-Prag D, Wang XF, Nizol L, Iannaccone A, Musch DC, Bush RA, Salem N Jr, Sieving PA, Ayyagari R. Elovl4 5-bp-deletion knock-in mice develop progressive photoreceptor degeneration. Invest Ophthalmol Vis Sci 2006;47:4558–4568. [PubMed: 17003453]

Vasireddy V, Uchida Y, Salem N Jr, Kim SY, Mandal MN, Reddy GB, Bodepudi R, Alderson NL, Brown JC, Hama H, Dlugosz A, Elias PM, Holleran WM, Ayyagari R. Loss of functional ELOVL4 depletes very long-chain fatty acids (> or =C28) and the unique omega-O-acylceramides in skin leading to neonatal death. Hum Mol Genet 2007;16:471–482. [PubMed: 17208947]

von Ruckmann A, Fitzke FW, Bird AC. In vivo fundus autofluorescence in macular dystrophies. Arch Ophthalmol 1997;115:609–615. [PubMed: 9152128]

Wabbels B, Preising MN, Kretschmann U, Demmler A, Lorenz B. Genotype-phenotype correlation and longitudinal course in ten families with Best vitelliform macular dystrophy. Graefes Arch Clin Exp Ophthalmol 2006;244:1453–1466. [PubMed: 16612637]

Wang Y, Meyer JW, Ashraf M, Shull GE. Mice with a null mutation in the NHE1 Na+-H+ exchanger are resistant to cardiac ischemia-reperfusion injury. Circ Res 2003;93:776–782. [PubMed: 12970112]

Wangsa-Wirawan ND, Linsenmeier RA. Retinal oxygen: fundamental and clinical aspects. Arch Ophthalmol 2003;121:547–557. [PubMed: 12695252]

Weingeist TA, Kobrin JL, Watzke RC. Histopathology of Best's macular dystrophy. Arch Ophthalmol 1982;100:1108–1114. [PubMed: 7092654]

Weng J, Mata NL, Azarian SM, Tzekov RT, Birch DG, Travis GH. Insights into the function of Rim protein in photoreceptors and etiology of Stargardt's disease from the phenotype in abcr knockout mice. Cell 1999;98:13–23. [PubMed: 10412977]

White K, Marquardt A, Weber BH. VMD2 mutations in vitelliform macular dystrophy (Best disease) and other maculopathies. Hum Mutat 2000;15:301–308. [PubMed: 10737974]

Won J, Smith RS, Peachey NS, Wu J, Hicks WL, Naggert JK, Nishina PM. Membrane frizzled-related protein is necessary for the normal development and maintenance of photoreceptor outer segments. Vis Neurosci 2008;25:563–574. [PubMed: 18764959]

Wu J, Marmorstein AD, Peachey NS. Functional abnormalities in the retinal pigment epithelium of CFTR mutant mice. Exp Eye Res 2006;83:424–428. [PubMed: 16626699]

Wu J, Marmorstein AD, Striessnig J, Peachey NS. Voltage-dependent calcium channel CaV1.3 subunits regulate the light peak of the electroretinogram. J Neurophysiol 2007;97:3731–3735. [PubMed: 17376851]

Wu J, Peachey NS, Marmorstein AD. Light-evoked responses of the mouse retinal pigment epithelium. J Neurophysiol 2004;91:1134–1142. [PubMed: 14614107]

Xiao Q, Prussia A, Yu K, Cui YY, Hartzell HC. Regulation of bestrophin Cl channels by calcium: role of the C terminus. J Gen Physiol 2008;132:681–692. [PubMed: 19029375]

Xiao XH, Allen DG. Role of Na(+)/H(+) exchanger during ischemia and preconditioning in the isolated rat heart. Circ Res 1999;85:723–730. [PubMed: 10521246]

Xiao XH, Allen DG. Activity of the Na(+)/H(+) exchanger is critical to reperfusion damage and preconditioning in the isolated rat heart. Cardiovasc Res 2000;48:244–253. [PubMed: 11054471]

Yang YD, Cho H, Koo JY, Tak MH, Cho Y, Shim WS, Park SP, Lee J, Lee B, Kim BM, Raouf R, Shin YK, Oh U. TMEM16A confers receptor-activated calcium-dependent chloride conductance. Nature 2008;455:1210–1215. [PubMed: 18724360]

Yao H, Gu XQ, Haddad GG. The role of HCO3(-)-dependent mechanisms in pHi regulation during O2 deprivation. Neuroscience 2003;117:29–35. [PubMed: 12605889]

Yao H, Haddad GG. Calcium and pH homeostasis in neurons during hypoxia and ischemia. Cell Calcium 2004;36:247–255. [PubMed: 15261480]

Yardley J, Leroy BP, Hart-Holden N, Lafaut BA, Loeys B, Messiaen LM, Perveen R, Reddy MA, Bhattacharya SS, Traboulsi E, Baralle D, De Laey JJ, Puech B, Kestelyn P, Moore AT, Manson FD, Black GC. Mutations of VMD2 splicing regulators cause nanophthalmos and autosomal dominant vitreoretinochoroidopathy (ADVIRC). Invest Ophthalmol Vis Sci 2004;45:3683–3689. [PubMed: 15452077]

Yu K, Cui Y, Hartzell HC. The bestrophin mutation A243V, linked to adult-onset vitelliform macular dystrophy, impairs its chloride channel function. Invest Ophthalmol Vis Sci 2006;47:4956–4961. [PubMed: 17065513]

Yu K, Xiao Q, Cui G, Lee A, Hartzell HC. The best disease-linked Cl- channel hBest1 regulates Ca V 1 (L-type) Ca2+ channels via src-homology-binding domains. J Neurosci 2008;28:5660–5670. [PubMed: 18509027]

Zhang Y, Davidson BR, Stamer WD, Barton JK, Marmorstein L, Marmorstein AD. Enhanced inflow and outflow rates despite lower IOP in Bestrophin-2 deficient mice. Invest Ophthalmol Vis Sci. 2008

Zhou D, Xue J, Chen J, Morcillo P, Lambert JD, White KP, Haddad GG. Experimental selection for Drosophila survival in extremely low O2 environment. PLoS ONE 2007;2:e490. [PubMed: 17534440]

Zhou D, Xue J, Gavrialov O, Haddad GG. Na+/H+ exchanger 1 deficiency alters gene expression in mouse brain. Physiol Genomics 2004;18:331–339. [PubMed: 15306696]

Zhuk SA, Edwards AO. Peripherin/RDS and VMD2 mutations in macular dystrophies with adult-onset vitelliform lesion. Mol Vis 2006;12:811–815. [PubMed: 16885924]

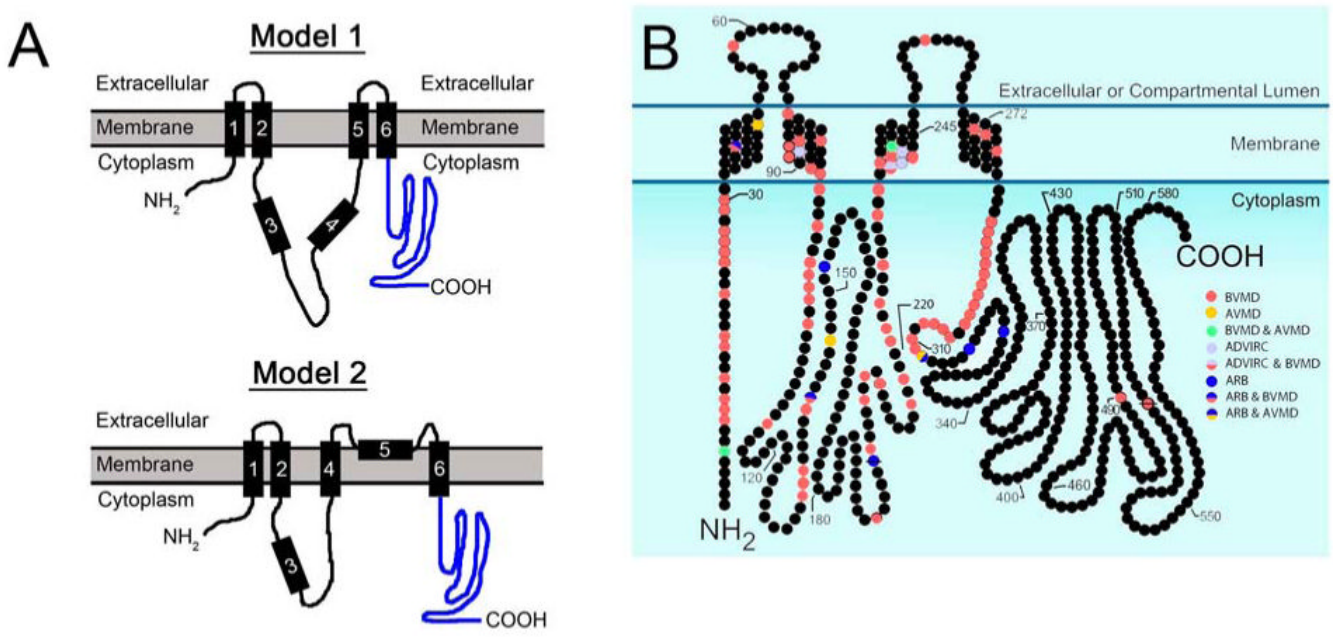

Figure 1.

Structure of hBest1. Best1 is integral membrane protein with 4-6 potential transmembrane spanning α-helices (numbered in A). There is general agreement that only 4 of these span the plasma membrane. Two models have been proposed. Model 1 is supported by the experimental data of (Milenkovic et al., 2007). Model 2 was proposed by and is supported experimentally by (Tsunenari et al., 2003). Through the years most investigators have favored model 1 because it is most frequently predicted by various protein structural software packages. There is no direct experimental data however, that should cause us to favor either model. In hBest1, there are 585 amino acids which are indicated by circles according to model 1 in B. Mutation sites and the human disease(s) they cause are indicated by colored circles. Using model 1, most disease causing mutations are clustered in regions adjacent to the cytosolic face of the 4 TM domains (B). The RFP-TM or bestrophin domain extends from the N-terminus through approximately amino acid 350 and contains all of the TM domains as well as nearly all reported disease causing mutations.

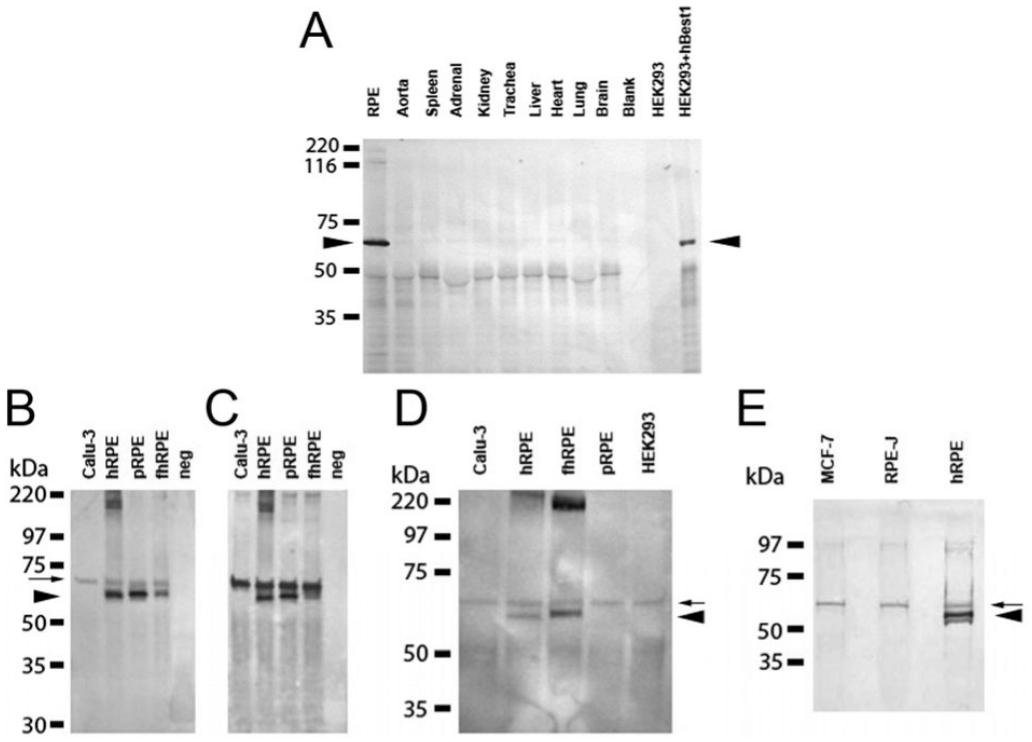

Figure 2.

Characterization of anti-hBest1 antibodies and expression of hBest1 in pig tissues, RPE, and cell lines. Lysates were prepared from porcine tissues or cultured cell lines as described in Marmorstein *et al.*, (2002). Immunoprecipiates were prepared from tissue lysates containing 1 gram of total protein as described in Marmorstein *et al.*, (2002) and pBest1 identified in those immunoprecipitates using monoclonal antibody E6-1 (A). Note pBest1 is present only in RPE (Arrow in A) and in no other tissue. hBest1 was expressed in HEK293 cells as a control, with untransfected HEK293 cell lysates serving as a negative control. Immunoprecipitates were prepared from lysates using polyclonal anti-hBest1 antibody Pab-125 for blots shown in B-D. Lysates were prepared from human RPE (hRPE) from a single donor eye, porcine RPE (pRPE) from a single donor eye, 2 × 1 cm^2 monolayers of cultured fetal human RPE (fhRPE), or a confluent well from a 12-well plate of Calu-3, MCF-7, HEK293, or RPE-J. Immunoprecipitates were resolved by SDS-Page, transferred to PVDF and hBest1 identified using monoclonal anti-hbest1 antibodies E6-1 (B), E6-6 (C, E), or 1C2 (D). Authentic hBest1 is indicated by an arrowhead, and a non-specific band with a slightly higher Mr is indicated with a small arrow. We could not detect hBest1 in the human cell lines Calu-3, HEK293, MCF-7 or the rat derived RPE cell line RPE-J. The absence of the higher Mr band from negative control lanes loaded with SDS-PAGE buffer only indicates that this non-specific band is recognized by all antibodies generated against the C-terminus of hBest1. Note that 1C2 does not recognize pBest1.

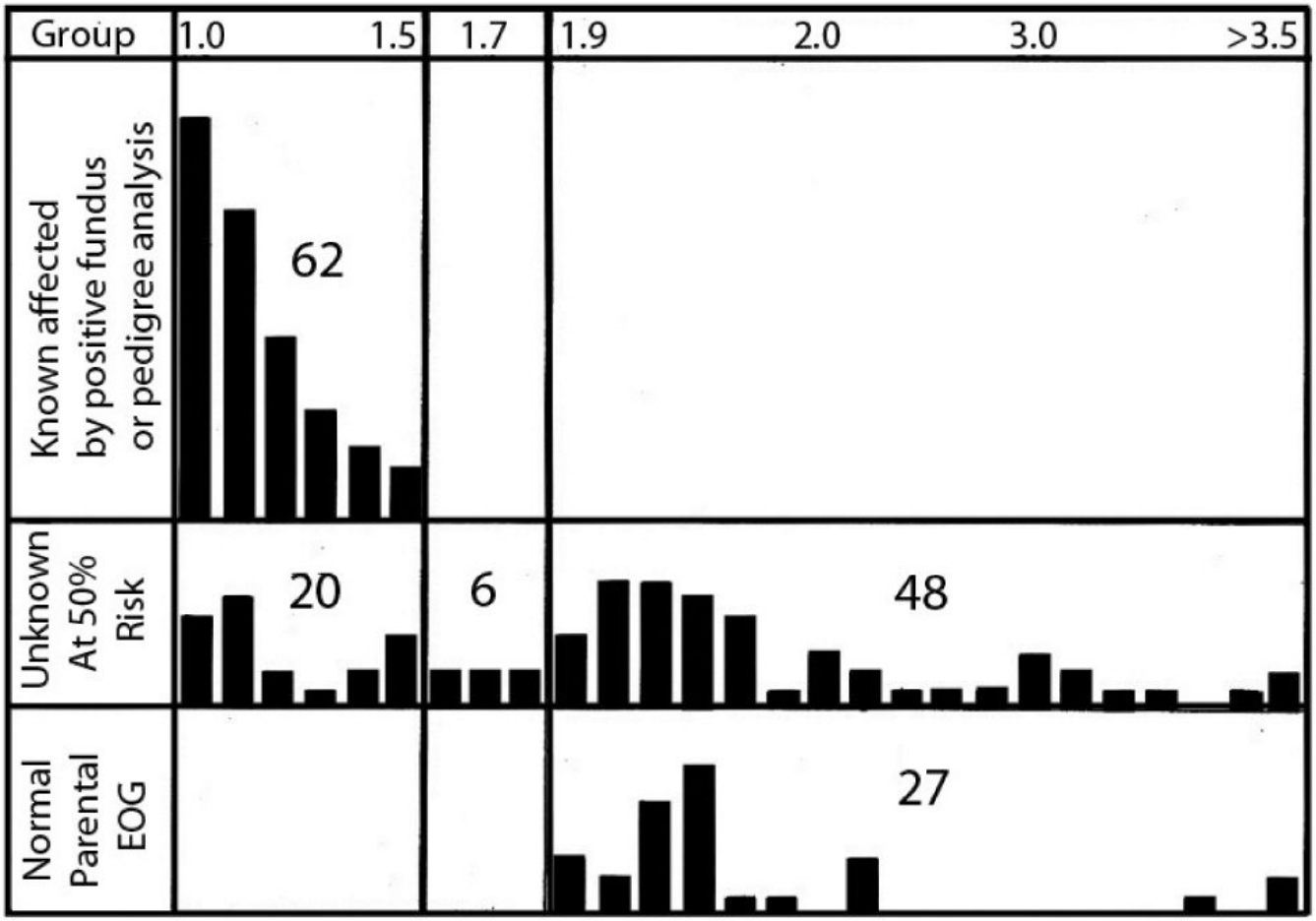

Figure 3.
EOG light/dark ratios in 163 eyes in families with BVMD. The ratio is indicated at the top and the total number of eyes within the boxes. From Bard and Cross (1975), Reproduced by permission of the University of Wisconsin Press.

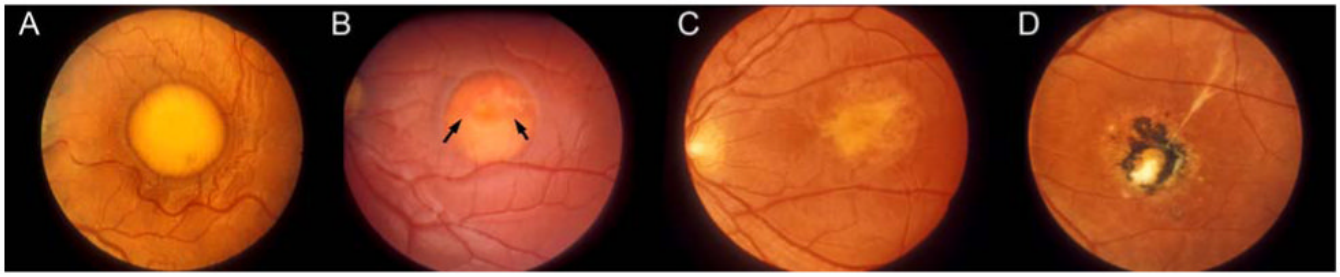

Figure 4.
Clinical progression of the fundus in BVMD. Classical vitelliform or stage IIa lesion is shown in A. Stage IIb is characterized by a visible fluid line (arrows) within the lesion (B). Partial resorption of the fluid within the lesion gives the appearance of a scrambled egg and is characteristic of Stage III or pseudohypopyon (C). Stage IV (D) is characterized by a gliotic scar accompanied by regions of hypo (stage IVa) or hyperpigmentation (stage IVb) and occasionally neovascularization (stage IVc).

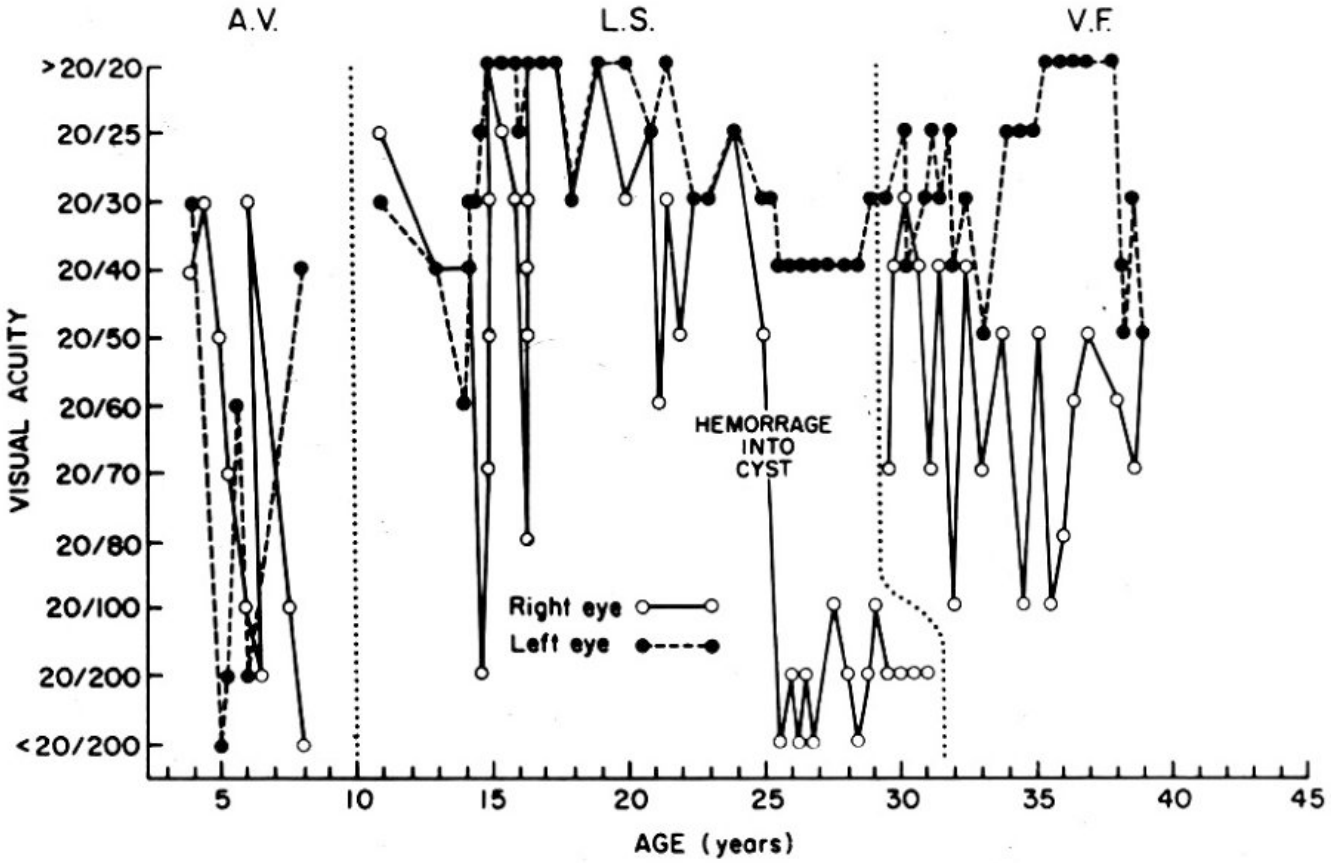

Figure 5.
Fluctuations in visual acuity in 3 patients with BVMD. From Bard and Cross (1975), Reproduced by permission of the University of Wisconsin Press.

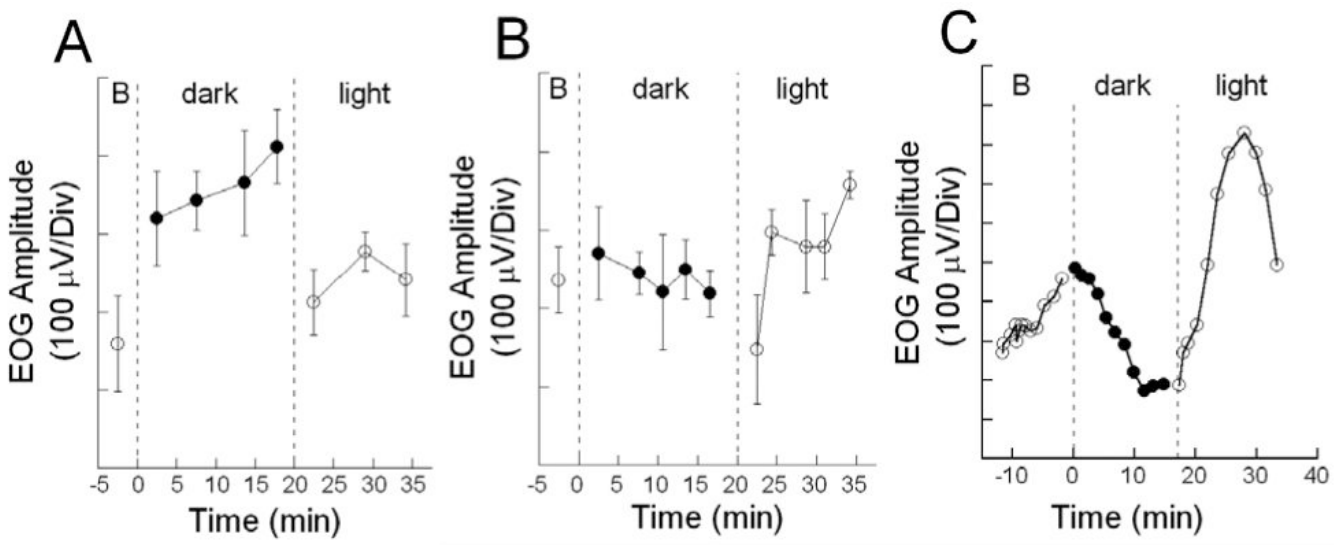

Figure 6.

Amplitude of EOG records obtained from a Sprague-Dawley rat (A), a Long-Evans rat (B) or a normal human subject (C) during the course of an experimental session in which the adaptation state of the eye was varied from room light level, to darkness (dark), to a steady stimulus (light). Note that the human EOG response increases during light exposure and decreases during darkness, whereas the rat responses have the opposite pattern (A) or are not modulated by light level. Data points in A and B reflect the average ± s.d. of at least 5 individual rats. Data points in C reflect individual measurements.

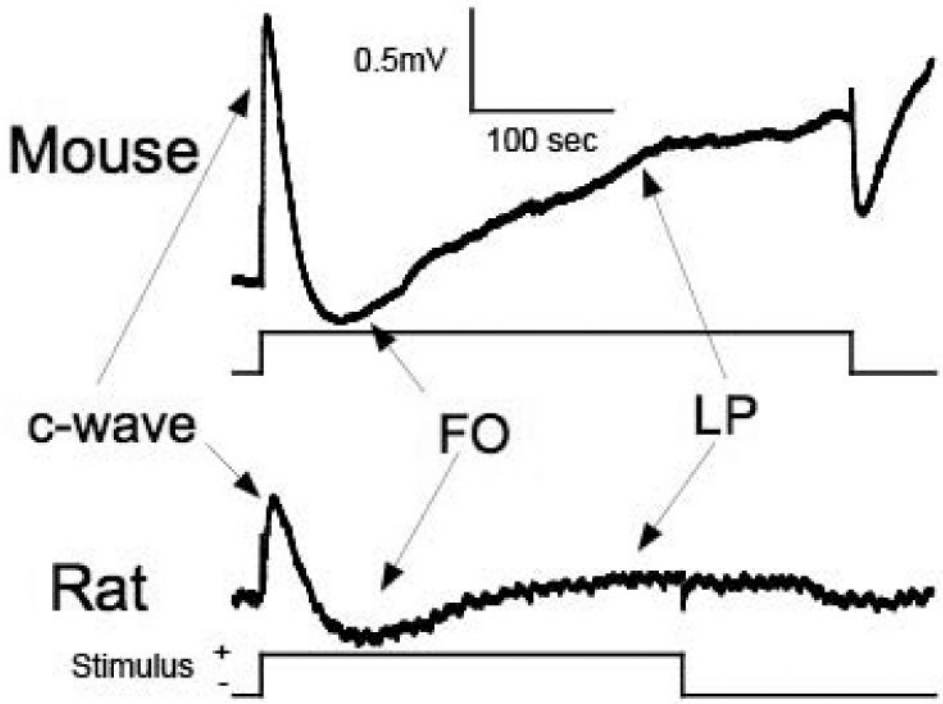

Figure 7.

dc-ERGs recorded from a WT mouse (upper waveform) or rat (lower waveform) in response to 7-minute (mouse) or 5-minute (rat) 2.4 log cd/m^2 stimuli. Note that each response includes all of the major dc-ERG components, and that the overall mouse response has larger amplitude.

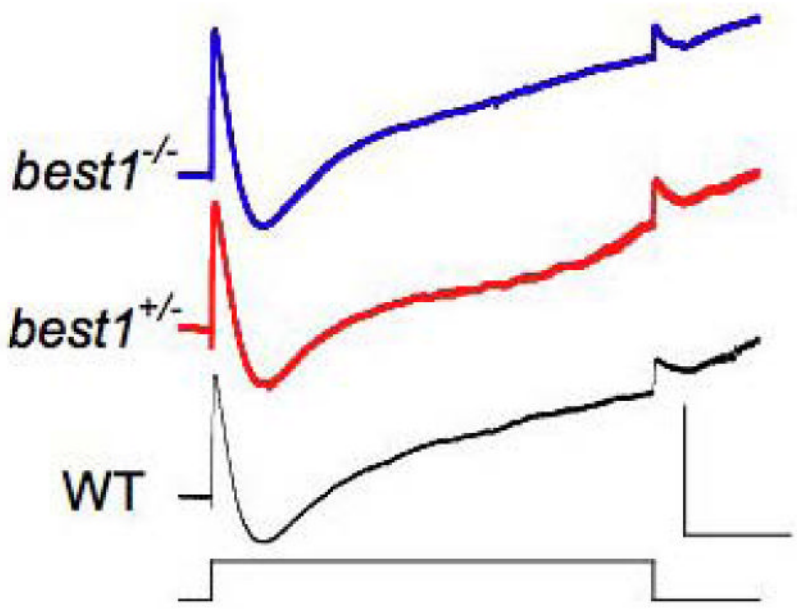

Figure 8.
dc-ERGs recorded from WT, Best1$^{+/-}$ and Best1$^{-/-}$ mice in response to a 7-minute 2.4 log cd/m^2 stimulus. Note that each response includes all of the major dc-ERG components.

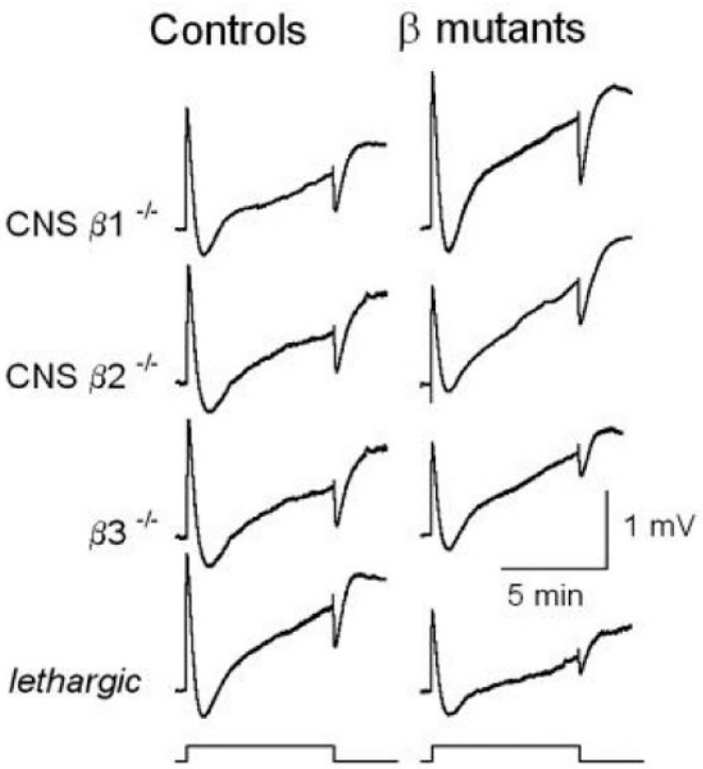

Figure 9.

dc-ERGs recorded from control mice (left column) or from mice lacking one of the four VDCC β subunits (right column) in response to 7-minute 2.4 log cd/m^2 stimuli. Note that the LP is reduced only in *lethargic* mice, lacking a functional β_4 subunit.

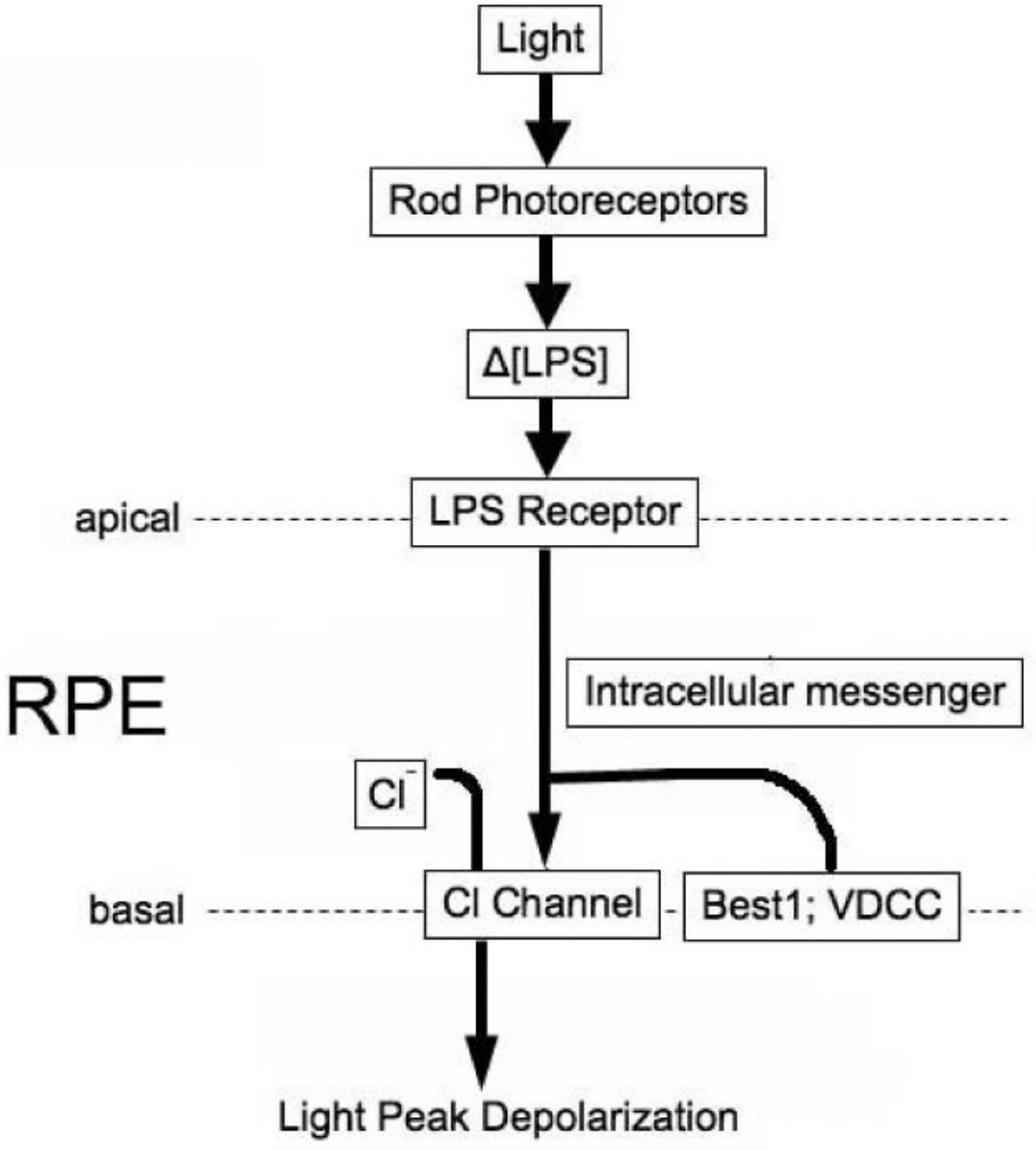

Figure 10.
Diagram of LP generation. Light-activation of rod photoreceptors alters the concentration of the unidentified *LPS* in the subretinal space. This change is detected by *LPS* receptors located on the apical RPE membrane. These receptors initiate an intracellular signal, which is modulated by Best1 and VDCCs, which ultimately increases the conductance of Cl^- channels, depolarizing the RPE cell. The depolarization event is recorded as the dc-ERG LP.

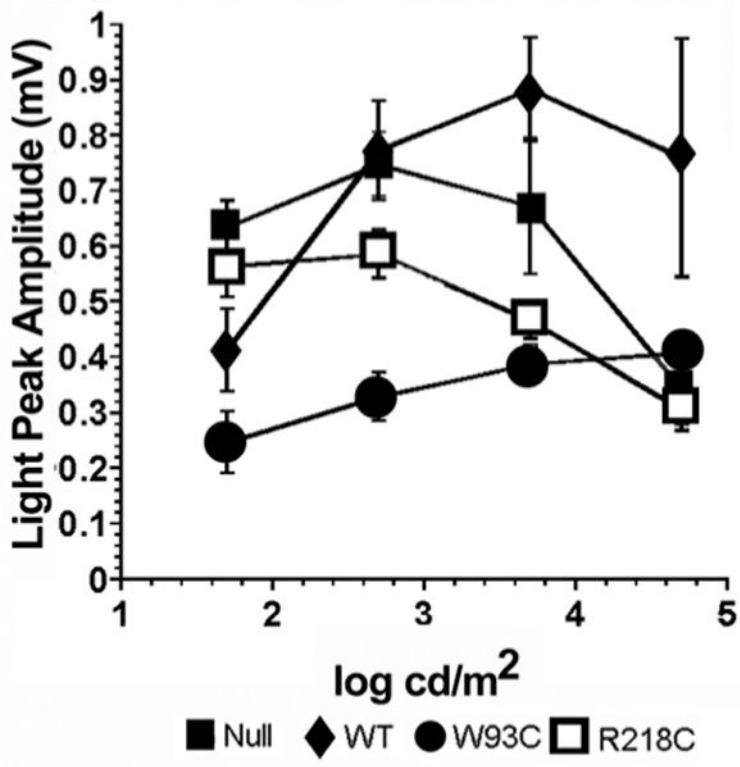

Figure 11.

Effect of hBest1 on rat LP amplitudes and luminance response. RPE generated ERG components were recorded in response to increasing luminance in rats injected subretinally with replication defective adenovirus vectors with an empty expression cassette (Null) or driving expression of hBest1 (WT), hBest1^{W93C} (W93C) or hBest1^{R218C} (R218C). Data indicate mean ± s.e.m. of 4 – 12 measurements.

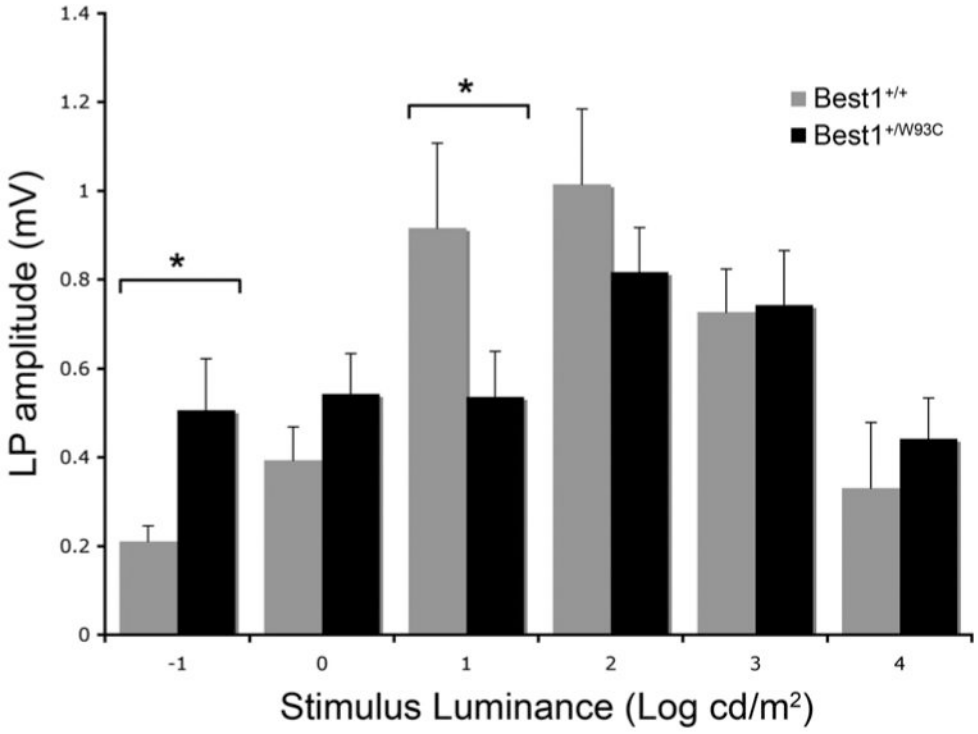

Figure 12.

LP amplitudes in *Best1*$^{+/W93C}$ KI mice. Dc-ERGs were recorded from *Best1*$^{+/W93C}$ knock-in mice or *Best1*$^{+/+}$ littermates in response to a 7 minute light stimulus varying over a 5 log range. Note that the LP amplitude in *Best1*$^{+/W93C}$ mice did not vary between -1 and +1 log cd/m^2. Significant differences ($p < 0.05$, indicated by *) were observed at -1 log cd/m^2 and at 1 log cd/m^2. The absolute maximum was obtained from both groups at 2 log cd/m^2. Although the average response at 2 log cd/m^2 was lower in *Best1*$^{+/W93C}$ mice than in *Best1*$^{+/+}$ mice, the difference was not statistically significant. Data shown are mean ± SE of the maximum LP amplitudes obtained at each stimulus luminance from 5-12 mice.

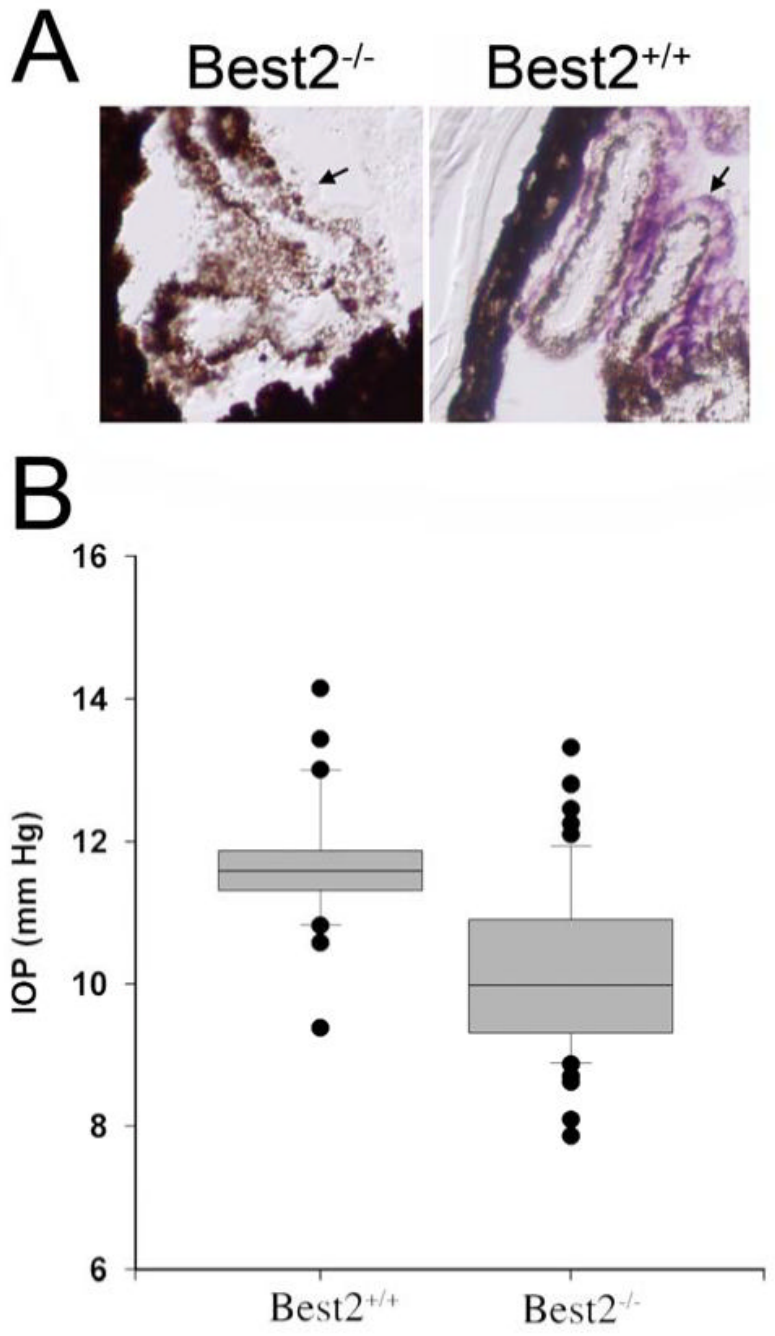

Figure 13.

Localization of mBest2 to the NPE and effect on IOP. The localization of mBest2 in the mouse eye was determined using immunohistochemistry (A). *Best2*$^{-/-}$ mice served as a control for antibody specificity. In the eye, the purple VIP reaction product indicating the presence of mBest2 was identified only in NPE cells (indicated by arrows in A) of wild type (*Best2*$^{+/+}$) mice. Based on this localization we compared the IOP of *Best2*$^{-/-}$ mice with *Best2*$^{+/+}$ mice (B). IOP was measured via anterior chamber cannulation. Note that IOP is significantly ($p < 0.0001$) lower in *Best2*$^{-/-}$ mice. Data are presented as a box plot in which the line within the box marks the median IOP, and the boundaries of the box indicate the range covered by the middle 50% of measurements. Bars above and below the boxes indicate the 90th and 10th percentiles

respectively. Symbols outside of the box and bars are outliers. For *Best2*$^{+/+}$ n = 31, for *Best2*$^{-/-}$ n= 55.

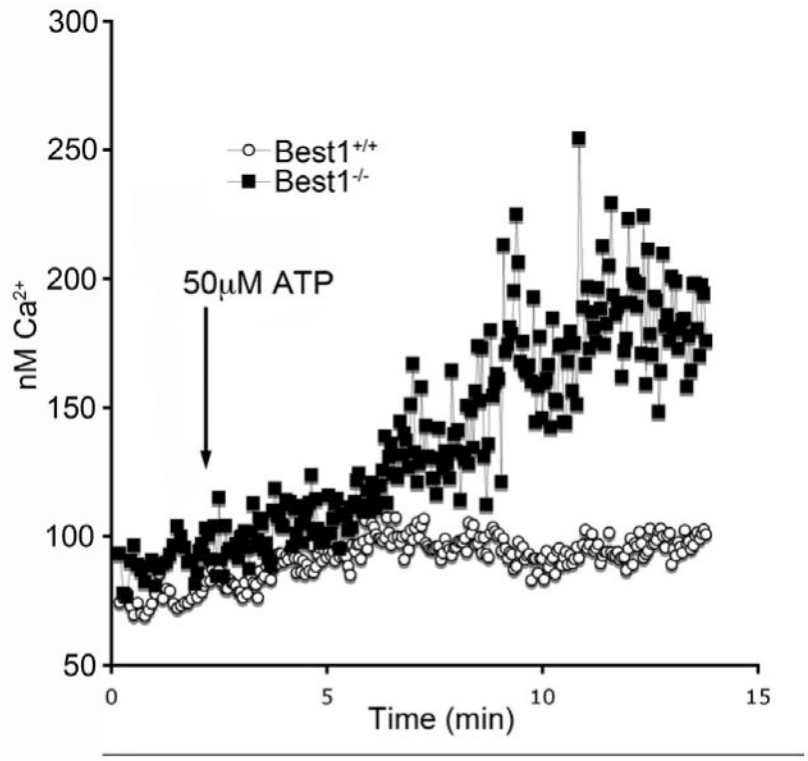

Figure 14.

Comparison of the change in intracellular Ca^{2+} concentration elicited by 50 mM ATP in RPE sheets isolated from $Best1^{+/+}$ or $Best1^{-/-}$ mice. Note that the increase in Ca^{2+} is much greater in the $Best1^{-/-}$ mouse than in the $Best1^{+/+}$ mouse. This effect may underlie the increased LP amplitude observed in $Best1^{-/-}$ mice in response to lower intensity stimuli.

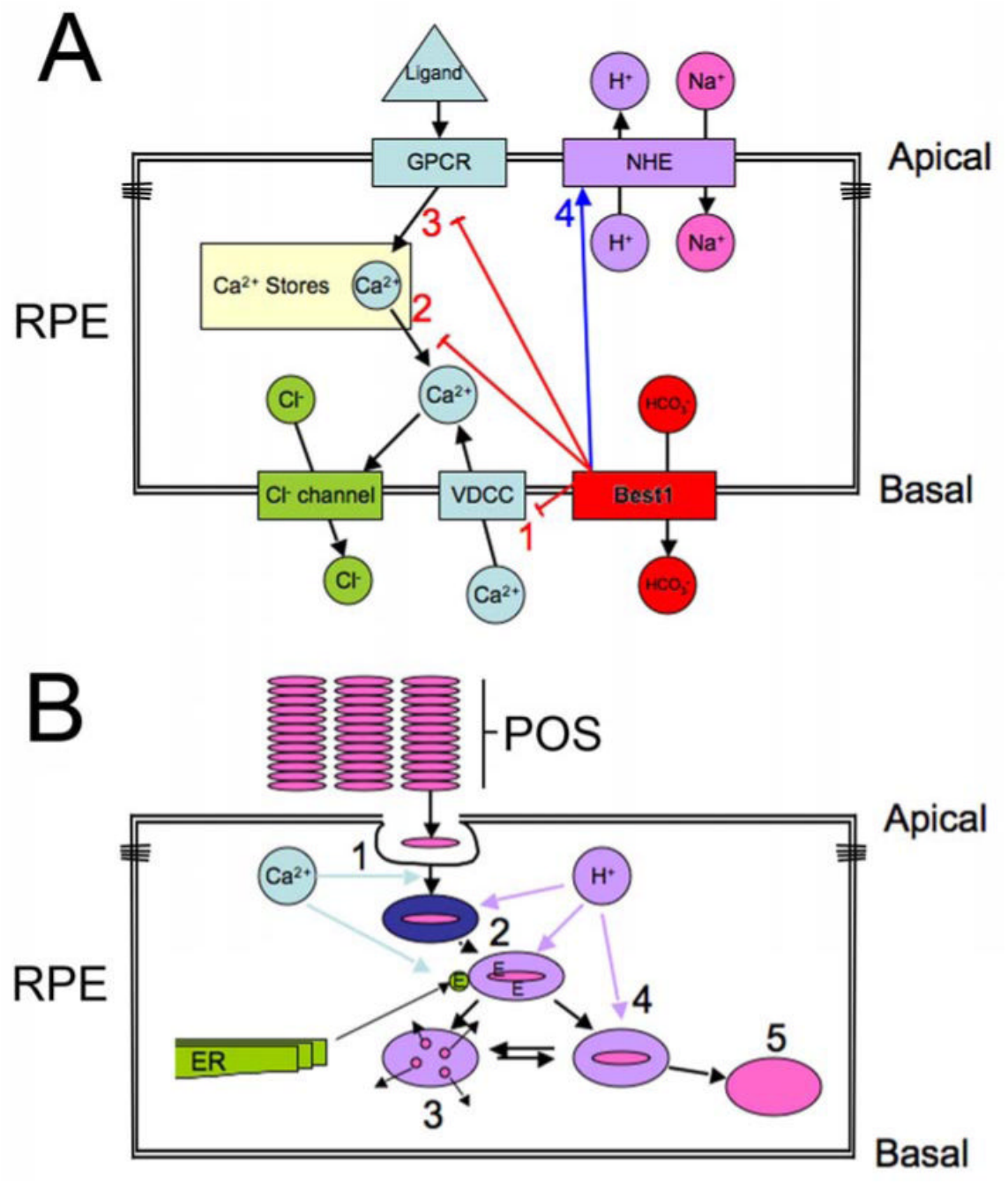

Figure 15.

Hypothetical model of Best1 function in the RPE. We propose that Best1 functions to set the gain on GPCR signaling via Ca^{2+} and to maintain intracellular pH in the face of a changing gradient of CO_2/HCO_3^- flowing across the RPE in response to changes in photoreceptor respiration. Combined data from several labs indicate that Best1 interacts physically and functionally with VDCCs (panel A, 1). The kinetic effects on VDCCs are to accelerate opening and closing times, resulting in a diminished entry of Ca^{2+}. Other effects on Ca^{2+} which we have identified in both $Best1^{W93C}$ knock-in, and $Best1^{-/-}$ mice as well as fhRPE cultures are the ability to modulate the release of Ca^{2+} stores in response to binding of a ligand to a GPCR (Panel A, 2 and 3). It is not clear yet whether this results form a block of store release (panel

A, 2) or by interference with GPCR signaling (panel A, 3). Best1 may be a channel protein. Although most investigators have examined its ability to conduct Cl-, it was recently found that Best1 was as or more efficient at conducting HCO_3^-. We have found that Best1 can alter pHi by promoting NHE activity (4). These effects appear to be dependent on HCO_3^-. It is likely that the changes in pH and Ca^{2+} due to Best1 activity are also interdependent. Should these functions be disrupted, we propose that the level of dysfunction dictates the disease phenotype (panel B). The common denominator in the bestrophinopathies is accumulation of lipofuscin, which could result from altered kinetics of phagocytosis uptake (panel B, 1), maturation (panel B, 2, 4), due to changes in acidification and / or delivery of lysosomal enzymes (E) (Panel B, 2). Under normal circumstances (Panel B, 3) the phagocytosed photoreceptor outer segment (POS) is properly degraded, however, a delay or acceleration in uptake, acidification, or degradation could promote the formation of A2E or other lipofuscin components from precursors already present in the POS. Liposufscin is non-degradable (Panel B, 4) and eventually accumulates in lipofuscin granules (5). The rate and level of lipofuscin accumulation would play a major role in the severity of the disease.